7 Maximally regular *T3*-type translational parallel robots

Maximally regular T3-type translational parallel robots are actuated by linear motors and can have various degrees of overconstraint. In these solutions, the three operational velocities are equal to their corresponding actuated joint velocities: $v_1 = \dot{q}_1$, $v_2 = \dot{q}_2$ and $v_3 = \dot{q}_3$. The Jacobian matrix in Eq. (1.19) is the identity matrix. We call *Isoglide3-T3* the translational parallel mechanisms of this family.

7.1 Overconstrained solutions

Equation (1.16) indicates that *overconstrained* solutions of maximally regular *T3*-type translational parallel robots with q independent loops meet the condition $\sum_1^p f_i < 3 + 6q$. Various solutions fulfil this condition along with $M_F = S_F = 3$ and $(R_F) = (\boldsymbol{v}_1, \boldsymbol{v}_2, \boldsymbol{v}_3)$. They may have identical limbs or limbs with different topologies. We limit our presentation in this section to the solutions with just three identical limbs.

7.1.1 Basic solutions with no idle mobilities

In the *basic* solutions of overconstrained maximally regular *T3*-type translational parallel robots, $F \leftarrow G_1$–G_2–G_3, the moving platform $n \equiv n_{Gi}$ ($i = 1, 2, 3$) is connected to the reference platform $1 \equiv 1_{Gi} \equiv 0$ by three simple or complex limbs with three (Figs. 7.1a, 7.2a–c) or four (Figs. 7.1b–e, 7.2d–k) degrees of connectivity. The complex limbs combine one (Fig. 7.2a, b, d–f, h–k) or two (Fig. 7.2c, g) planar closed loops of types *Pa* (Fig. 7.2a–e), *Rb* (Fig. 7.2f, g) *Pn2* (Fig. 7.2h, i) and *Pn3* (Fig. 7.2j, k). No idle mobilities exist in these basic solutions.

The planar loops with two and three degrees of freedom *Pn2*-type illustrated in Fig. 7.2h, i are of types $R||R||R||R$ and $R \perp P \perp^{||} R \perp P \perp^{||} R$. The planar loops with three degrees of freedom *Pn3*-type illustrated in

G. Gogu, *Structural Synthesis of Parallel Robots: Part 2: Translational Topologies with Two and Three Degrees of Freedom,* Solid Mechanics and Its Applications 159, 687–748.

Fig. 7.2j, k are of types $R||R||R||R||R$ and $R \perp P \perp^{||} R||R \perp P \perp^{||} R$. Other planar loops of types *Pn2* and *Pn3* can also be used (see Table 5.1).

Various solutions of maximally regular *T3*-type translational parallel robots with no idle mobilities can be obtained by using three limbs with identical or different topologies presented in Figs. 7.1 and 7.2. We only show solutions with identical limb type as illustrated in Figs. 7.3–7.13. The limb topologies and connecting conditions in these solutions are systematized in Table 7.1 and their structural parameters in Tables 7.2 and 7.3.

The limbs presented in Figs. 7.1 and 7.2 can also be used to generate basic solutions of overconstrained *T3*-type TPMs with uncoupled, decoupled and coupled motions.

Basic solutions of *T3*-type TPMs with *uncoupled motions* and different limb topologies can be obtained by using the following combinations of limbs: (i) one limb from Fig. 7.1 or 7.2 and two limbs from Figs. 5.1–5.5 or 6.1, (ii) two limbs from Fig. 7.2 or 7.3 and one limb from Figs. 5.1–5.5 or 6.1.

Basic solutions of *T3*-type TPMs with *decoupled motions* and different limb topologies can be obtained by using two limbs from Figs. 7.1 and 7.2 and one limb from Figs. 3.1–3.5, Figs. 3.60–3.70 and Figs. 4.1, 4.2 or 4.29.

Basic solutions of *T3*-type TPMs with *coupled motions* and different limb topologies can be obtained by using one limb from Fig. 7.1 or 7.2 and two limbs from Figs. 3.1–3.5, Figs. 3.60–3.70 and Figs. 4.1, 4.2 or 4.29.

Table 7.1. Limb topology and connecting conditions of the overconstrained maximally regular TPM with no idle mobilities presented in Figs. 7.3–7.13

No.	TPM type	Limb topology	Connecting conditions
1	*3-PPP* (Fig. 7.3a)	$\underline{P} \perp P \perp^{\perp} P$ (Fig. 7.1a)	The directions of the actuated prismatic joints are reciprocally orthogonal. The directions of the prismatic joints adjacent to the moving platform are also reciprocally orthogonal.
2	*3-PPP* (Fig. 7.3b, c)	$\underline{P} \perp P \perp^{\perp} P$ (Fig. 7.1a)	The directions of the actuated prismatic joints are reciprocally orthogonal. The directions of the prismatic joints adjacent to the moving platform are parallel to two orthogonal lines.
3	*3-PRRP* (Fig. 7.4a)	$\underline{P}\|\|R\|\|R \perp P$ (Fig. 7.1b)	Idem No. 1
4	*3-PRPR* (Fig. 7.4b)	$\underline{P}\|\|R \perp P \perp^{\|\|} R$ (Fig. 7.1c)	The directions of the actuated prismatic joints are reciprocally orthogonal.
5	*3-PPRR* (Fig. 7.5a)	$\underline{Pa} \perp Pa \perp^{\|\|} P$ (Fig. 7.1d)	Idem No. 4
6	*3-PRRR* (Fig. 7.5b)	$\underline{P}\|\|R\|\|R\|\|R$ (Fig. 7.1e)	Idem No. 4
7	*3-PPaP* (Fig. 7.6a)	$\underline{P}\|\|Pa \perp P$ (Fig. 7.2a)	Idem No. 1
8	*3-PPaP* (Fig. 7.6b)	$\underline{P}\|\|Pa \perp P$ (Fig. 7.2a)	Idem No. 2
9	*3-PPPa* (Fig. 7.7a, b)	$\underline{P} \perp P \perp^{\|\|} Pa$ (Fig. 7.2b)	Idem No. 4
10	*3-PPaPa* (Fig. 7.8a, b)	$\underline{P}\|\|Pa\|\|Pa$ (Fig. 7.2c)	Idem No. 4
11	*3-PRRPa* (Fig. 7.9a, b)	$\underline{P}\|\|R\|\|R\|\|Pa$ (Fig. 7.2d)	Idem No. 4
12	*3-PPaRR* (Fig. 7.10a, b)	$\underline{P}\|\|Pa\|\|R\|\|R$ (Fig. 7.2e)	Idem No. 4
13	*3-PRRbR* (Fig. 7.11a)	$\underline{P}\|\|R\|\|Rb\|\|R$ (Fig. 7.2f)	Idem No. 4
14	*3-PRRbRbR* (Fig. 7.11b)	$\underline{P}\|\|R\|\|Rb\|\|Rb\|\|R$ (Fig. 7.2g)	Idem No. 4
15	*3-PPn2R* (Fig. 7.12a, b)	$\underline{P}\|\|Pn2\|\|R$ (Fig. 7.2h, i)	Idem No. 4
15	*3-PPn3* (Fig. 7.13a, b)	$\underline{P}\|\|Pn3$ (Fig. 7.2j, k)	Idem No. 4

Table 7.2. Structural parameters[a] of translational parallel mechanisms in Figs. 7.3–7.7

No.	Structural parameter	Solution *3-PPP* (Fig. 7.3)	*3-PRRP*, *3-PRPR* (Fig. 7.4) *3-PPRR*, *3-PRRR* (Fig. 7.5)	*3-PPaP* (Fig. 7.6) *3-PPPa* (Fig. 7.7)
1	m	8	11	14
2	p_1	3	4	6
3	p_2	3	4	6
4	p_3	3	4	6
5	p	9	12	18
6	q	2	2	5
7	k_1	3	3	0
8	k_2	0	0	3
9	k	3	3	3
10	(R_{G1})	$(\boldsymbol{v}_1,\boldsymbol{v}_2,\boldsymbol{v}_3)$	$(\boldsymbol{v}_1,\boldsymbol{v}_2,\boldsymbol{v}_3,\omega_\alpha)$	$(\boldsymbol{v}_1,\boldsymbol{v}_2,\boldsymbol{v}_3)$
11	(R_{G2})	$(\boldsymbol{v}_1,\boldsymbol{v}_2,\boldsymbol{v}_3)$	$(\boldsymbol{v}_1,\boldsymbol{v}_2,\boldsymbol{v}_3,\omega_\beta)$	$(\boldsymbol{v}_1,\boldsymbol{v}_2,\boldsymbol{v}_3)$
12	(R_{G3})	$(\boldsymbol{v}_1,\boldsymbol{v}_2,\boldsymbol{v}_3)$	$(\boldsymbol{v}_1,\boldsymbol{v}_2,\boldsymbol{v}_3,\omega_\delta)$	$(\boldsymbol{v}_1,\boldsymbol{v}_2,\boldsymbol{v}_3)$
13	S_{G1}	3	4	3
14	S_{G2}	3	4	3
15	S_{G3}	3	4	3
16	r_{G1}	0	0	3
17	r_{G2}	0	0	3
18	r_{G3}	0	0	3
19	M_{G1}	3	4	3
20	M_{G2}	3	4	3
21	M_{G3}	3	4	3
22	(R_F)	$(\boldsymbol{v}_1,\boldsymbol{v}_2,\boldsymbol{v}_3)$	$(\boldsymbol{v}_1,\boldsymbol{v}_2,\boldsymbol{v}_3)$	$(\boldsymbol{v}_1,\boldsymbol{v}_2,\boldsymbol{v}_3)$
23	S_F	3	3	3
24	r_1	0	0	9
25	r_F	6	9	15
26	M_F	3	3	3
27	N_F	6	3	15
28	T_F	0	0	0
29	$\sum_{j=1}^{p_1} f_j$	3	4	6
30	$\sum_{j=1}^{p_2} f_j$	3	4	6
31	$\sum_{j=1}^{p_3} f_j$	3	4	6
32	$\sum_{j=1}^{p} f_j$	9	12	18

[a]See footnote of Table 2.1 for the nomenclature of structural parameters

Table 7.3. Structural parameters[a] of translational parallel mechanisms in Figs. 7.8–7.13

No.	Structural parameter	Solution *3-PPaPa* (Fig. 7.8)	*3-PRRPa* (Fig. 7.9) *3-PPaRR* (Fig. 7.10) *3-PRRbR* (Fig. 7.11a) *3-PPn2R* (Fig. 7.12a, b) *3-PPn3* (Fig. 7.13a, b)	*3-PRRbRbR* (Fig. 7.11b)
1	m	20	17	23
2	p_1	9	7	10
3	p_2	9	7	10
4	p_3	9	7	10
5	p	27	21	30
6	q	8	5	8
7	k_1	0	0	0
8	k_2	3	3	3
9	k	3	3	3
10	(R_{G1})	$(\boldsymbol{v}_1,\boldsymbol{v}_2,\boldsymbol{v}_3)$	$(\boldsymbol{v}_1,\boldsymbol{v}_2,\boldsymbol{v}_3,\boldsymbol{\omega}_\alpha)$	$(\boldsymbol{v}_1,\boldsymbol{v}_2,\boldsymbol{v}_3,\boldsymbol{\omega}_\alpha)$
11	(R_{G2})	$(\boldsymbol{v}_1,\boldsymbol{v}_2,\boldsymbol{v}_3)$	$(\boldsymbol{v}_1,\boldsymbol{v}_2,\boldsymbol{v}_3,\boldsymbol{\omega}_\beta)$	$(\boldsymbol{v}_1,\boldsymbol{v}_2,\boldsymbol{v}_3,\boldsymbol{\omega}_\beta)$
12	(R_{G3})	$(\boldsymbol{v}_1,\boldsymbol{v}_2,\boldsymbol{v}_3)$	$(\boldsymbol{v}_1,\boldsymbol{v}_2,\boldsymbol{v}_3,\boldsymbol{\omega}_\delta)$	$(\boldsymbol{v}_1,\boldsymbol{v}_2,\boldsymbol{v}_3,\boldsymbol{\omega}_\delta)$
13	S_{G1}	3	4	4
14	S_{G2}	3	4	4
15	S_{G3}	3	4	4
16	r_{G1}	6	3	6
17	r_{G2}	6	3	6
18	r_{G3}	6	3	6
19	M_{G1}	3	4	4
20	M_{G2}	3	4	4
21	M_{G3}	3	4	4
22	(R_F)	$(\boldsymbol{v}_1,\boldsymbol{v}_2,\boldsymbol{v}_3)$	$(\boldsymbol{v}_1,\boldsymbol{v}_2,\boldsymbol{v}_3)$	$(\boldsymbol{v}_1,\boldsymbol{v}_2,\boldsymbol{v}_3)$
23	S_F	3	3	3
24	r_1	18	9	18
25	r_F	24	18	27
26	M_F	3	3	3
27	N_F	24	12	21
28	T_F	0	0	0
29	$\sum_{j=1}^{p_1} f_j$	9	7	10
30	$\sum_{j=1}^{p_2} f_j$	9	7	10
31	$\sum_{j=1}^{p_3} f_j$	9	7	10
32	$\sum_{j=1}^{p} f_j$	27	21	30

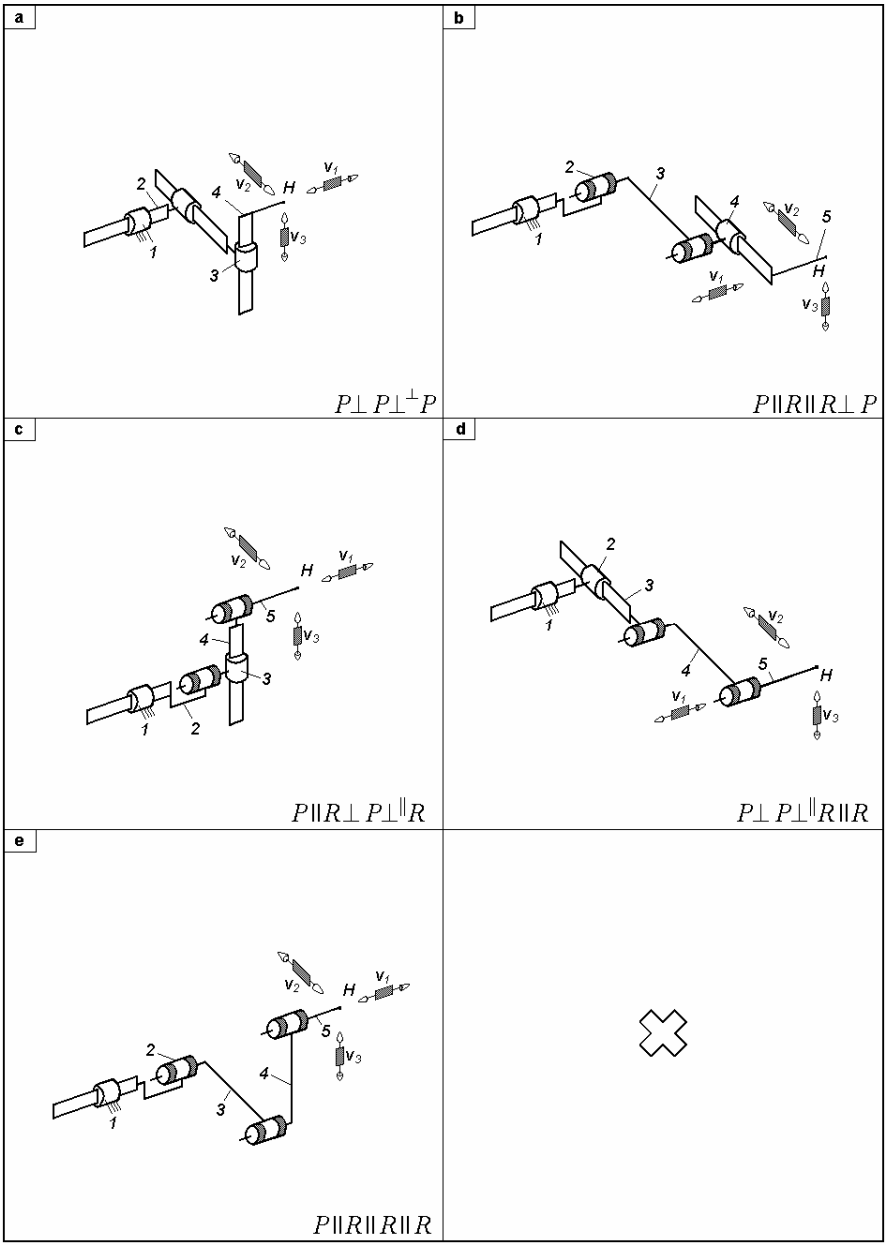

Fig. 7.1. Simple limbs for overconstrained maximally regular TPMs with no idle mobilities actuated by linear motors mounted on the fixed base, defined by $M_G = S_G = 3$, $(R_G) = (\boldsymbol{v}_1, \boldsymbol{v}_2, \boldsymbol{v}_3)$ – (**a**) and $M_G = S_G = 4$, $(R_G) = (\boldsymbol{v}_1, \boldsymbol{v}_2, \boldsymbol{v}_3, \boldsymbol{\omega}_\alpha)$ – (**b–e**)

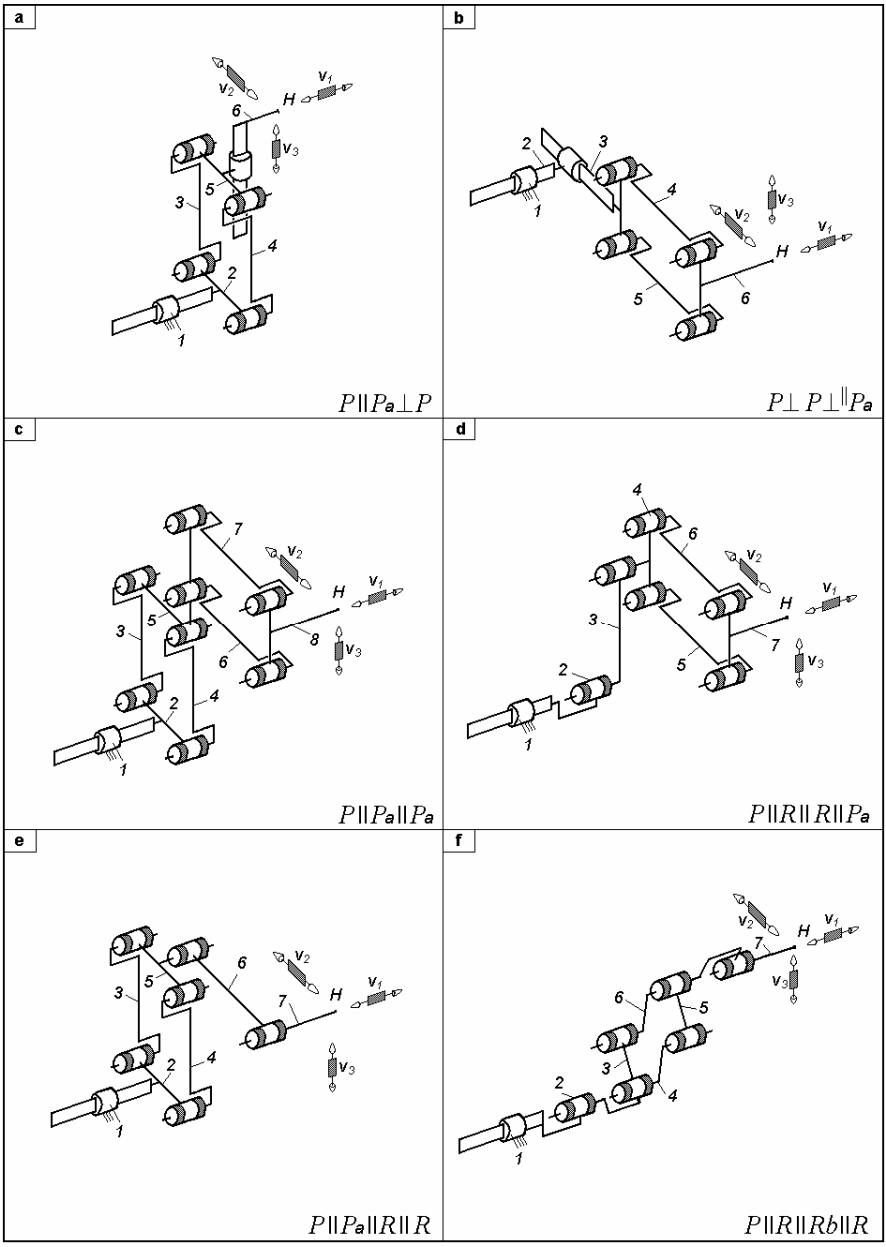

Fig. 7.2. Complex limbs for overconstrained maximally regular TPMs with no idle mobilities actuated by linear motors mounted on the fixed base, defined by $M_G = S_G = 3$, $(R_G) = (\boldsymbol{v}_1, \boldsymbol{v}_2, \boldsymbol{v}_3)$ – (**a**–**c**) and $M_G = S_G = 4$, $(R_G) = (\boldsymbol{v}_1, \boldsymbol{v}_2, \boldsymbol{v}_3, \boldsymbol{\omega}_\alpha)$ – (**d**–**k**)

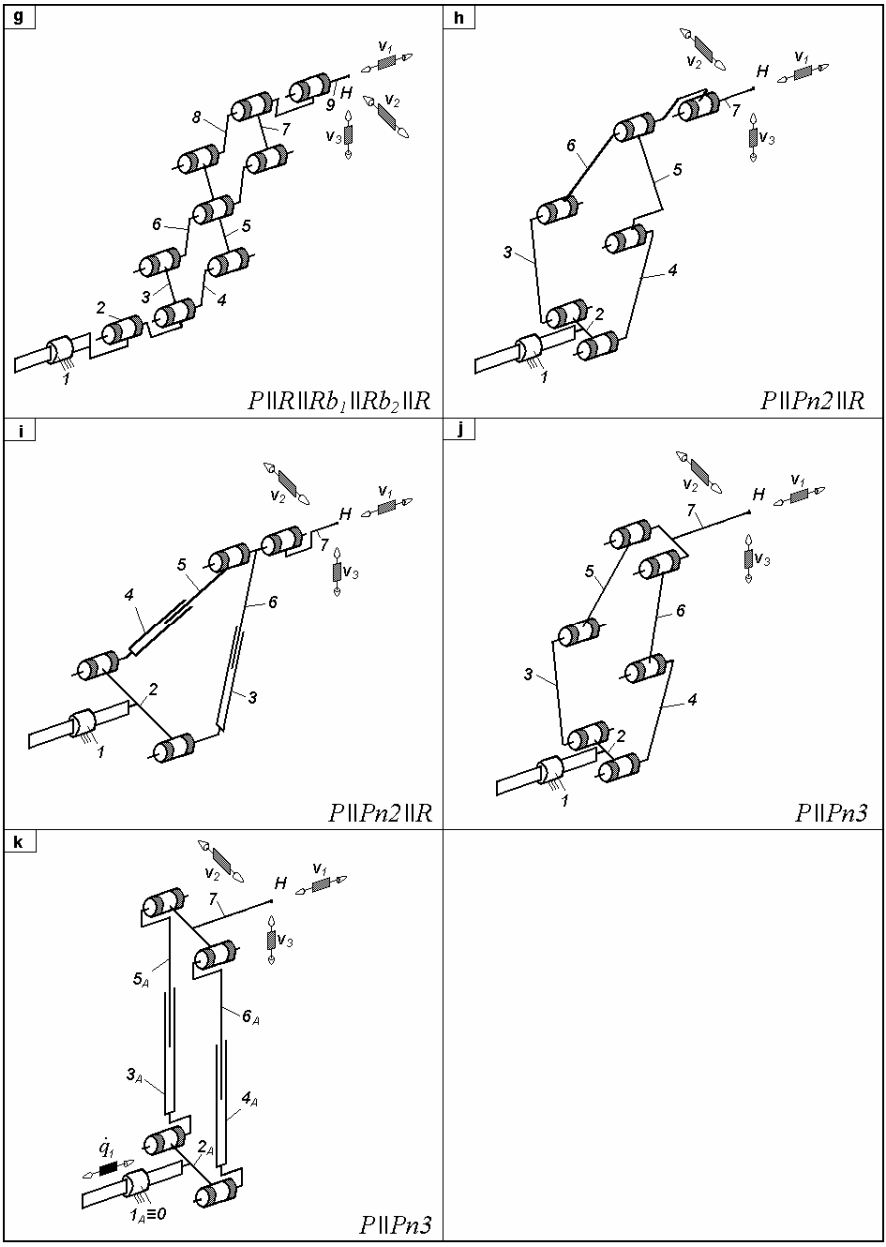

Fig. 7.2. (cont.)

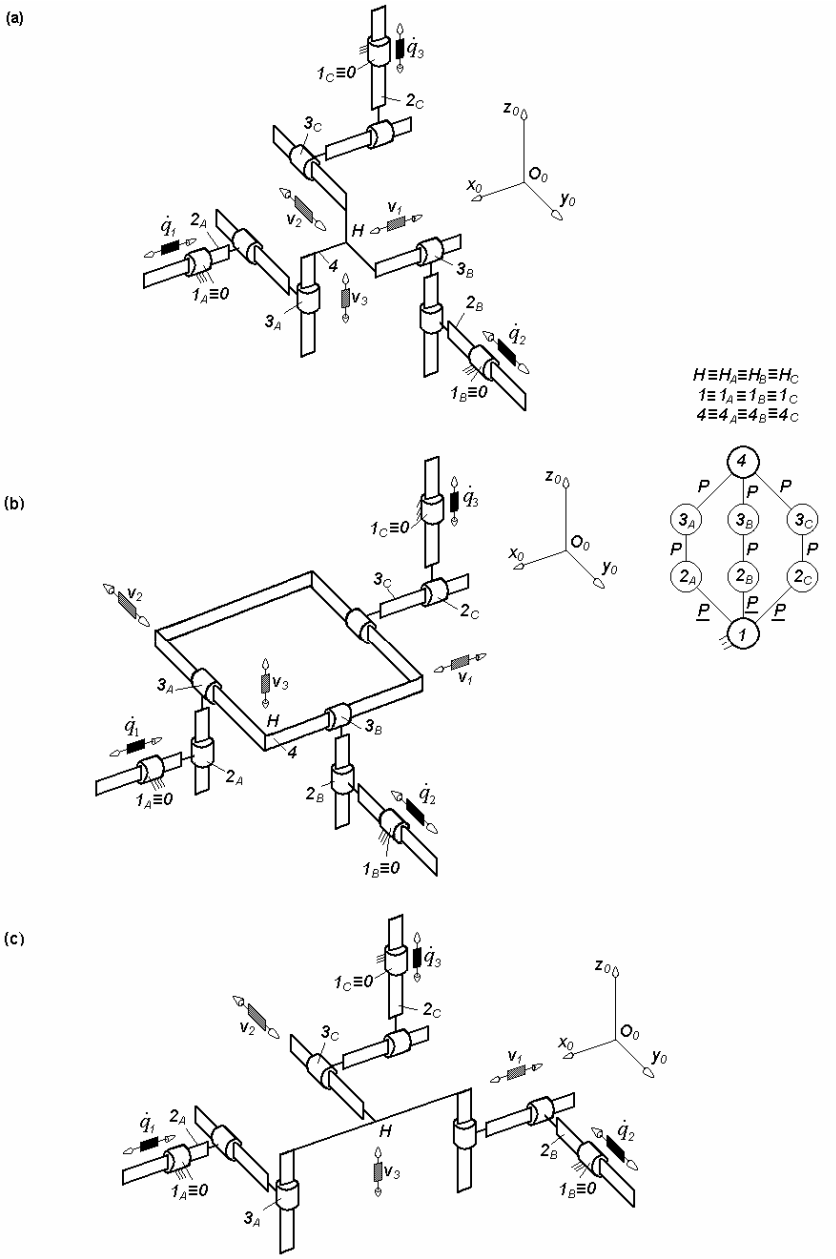

Fig. 7.3. *3-<u>P</u>PP*-type overconstrained maximally-regular TPMs defined by $M_F = S_F = 3$, $(R_F) = (\boldsymbol{v}_1, \boldsymbol{v}_2, \boldsymbol{v}_3)$, $T_F = 0$, $N_F = 6$, limb topology $\underline{P} \perp P \perp^{\perp} P$

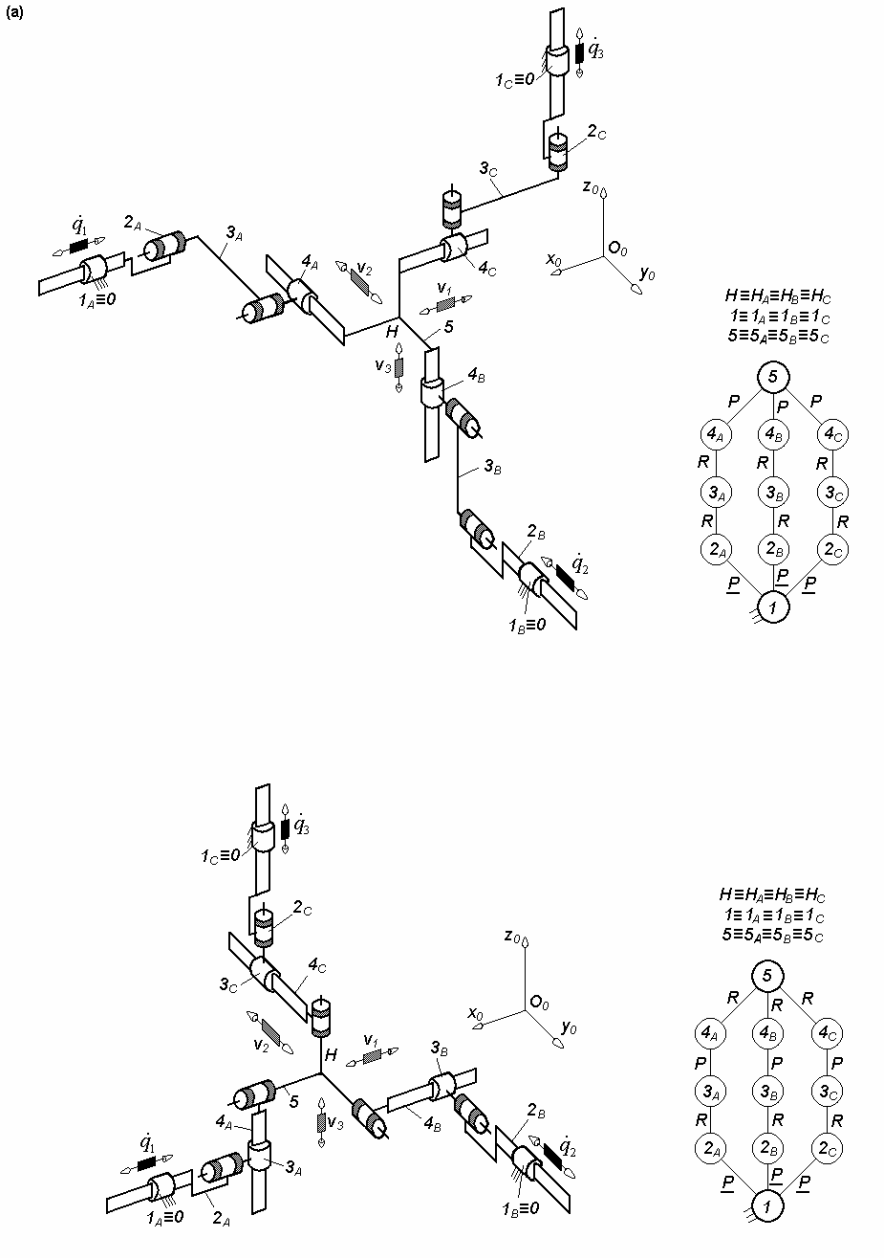

Fig. 7.4. Overconstrained maximally-regular TPMs of types *3-*$\underline{P}$*RRP* (**a**) and *3-*$\underline{P}$*RPR* (**b**) defined by $M_F = S_F = 3$, $(R_F) = (\boldsymbol{v}_1, \boldsymbol{v}_2, \boldsymbol{v}_3)$, $T_F = 0$, $N_F = 3$, limb topology $\underline{P}||R||R \perp P$ (**a**) and $\underline{P}||R \perp P \perp {}^{||}R$ (**b**)

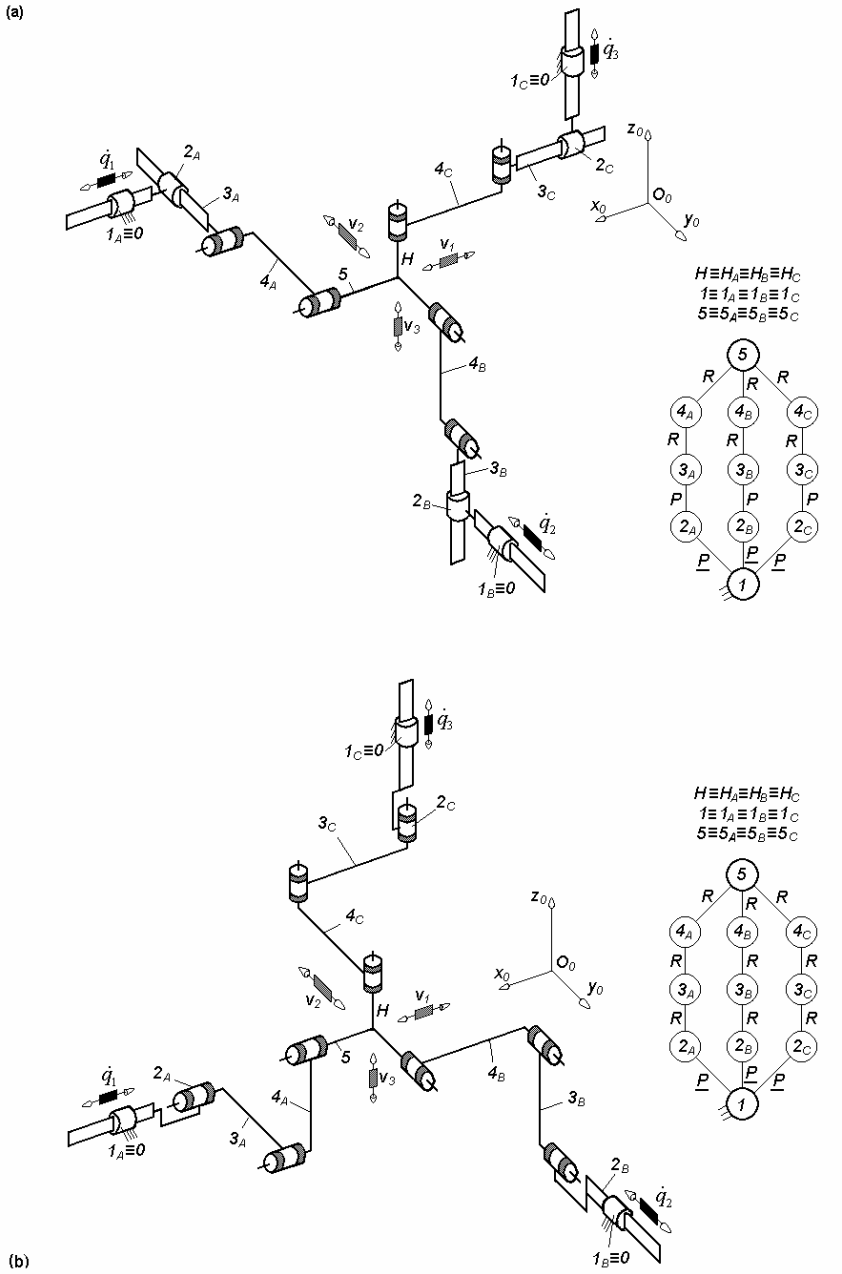

Fig. 7.5. Overconstrained maximally-regular TPMs of types *3-*$\underline{P}$*PRR* (**a**) and *3-*$\underline{P}$*RRR* (**b**) defined by $M_F = S_F = 3$, $(R_F) = (\boldsymbol{v}_1, \boldsymbol{v}_2, \boldsymbol{v}_3)$, $T_F = 0$, $N_F = 3$, limb topology $\underline{P} \perp P \perp {}^{\parallel}R||R$ (**a**) and $\underline{P}||R||R||R$ (**b**)

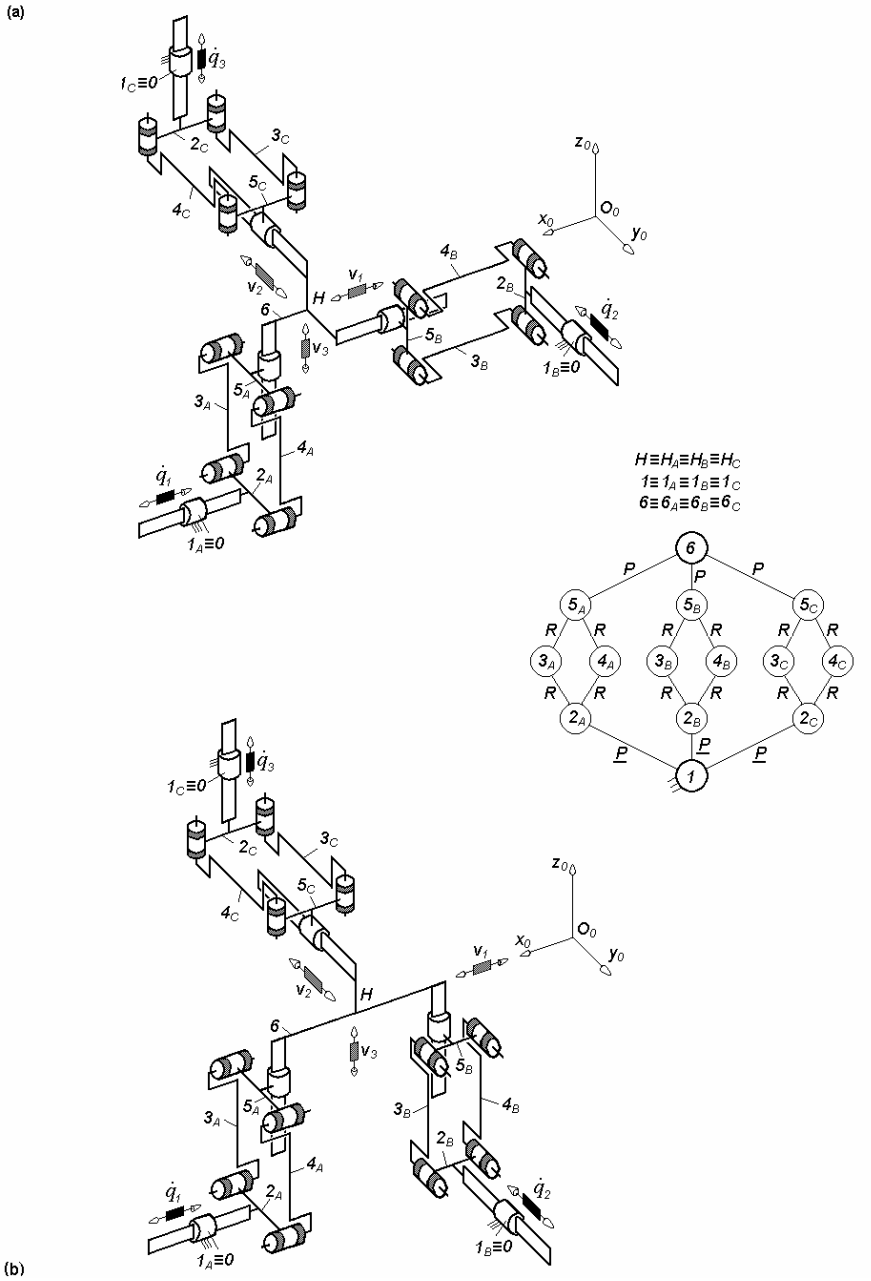

Fig. 7.6. *3-PPaP*-type overconstrained maximally-regular TPMs defined by $M_F = S_F = 3$, $(R_F) = (\boldsymbol{v}_1, \boldsymbol{v}_2, \boldsymbol{v}_3)$, $T_F = 0$, $N_F = 15$, limb topology $\underline{P}||Pa \perp P$

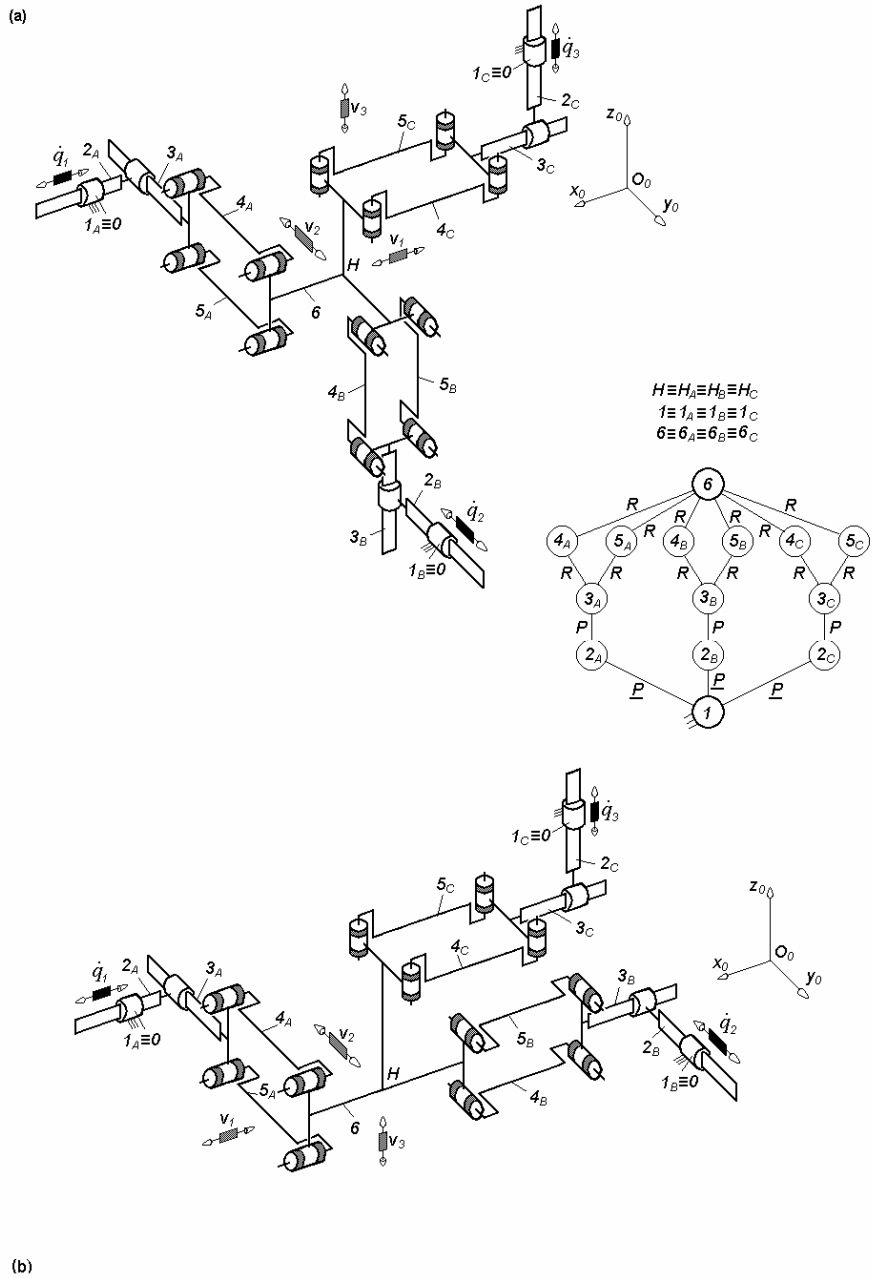

Fig. 7.7. *3-<u>P</u>PPa*-type overconstrained maximally-regular TPMs defined by $M_F = S_F = 3$, $(R_F) = (\boldsymbol{v}_1, \boldsymbol{v}_2, \boldsymbol{v}_3)$, $T_F = 0$, $N_F = 15$, limb topology $\underline{P} \perp P \perp \parallel Pa$

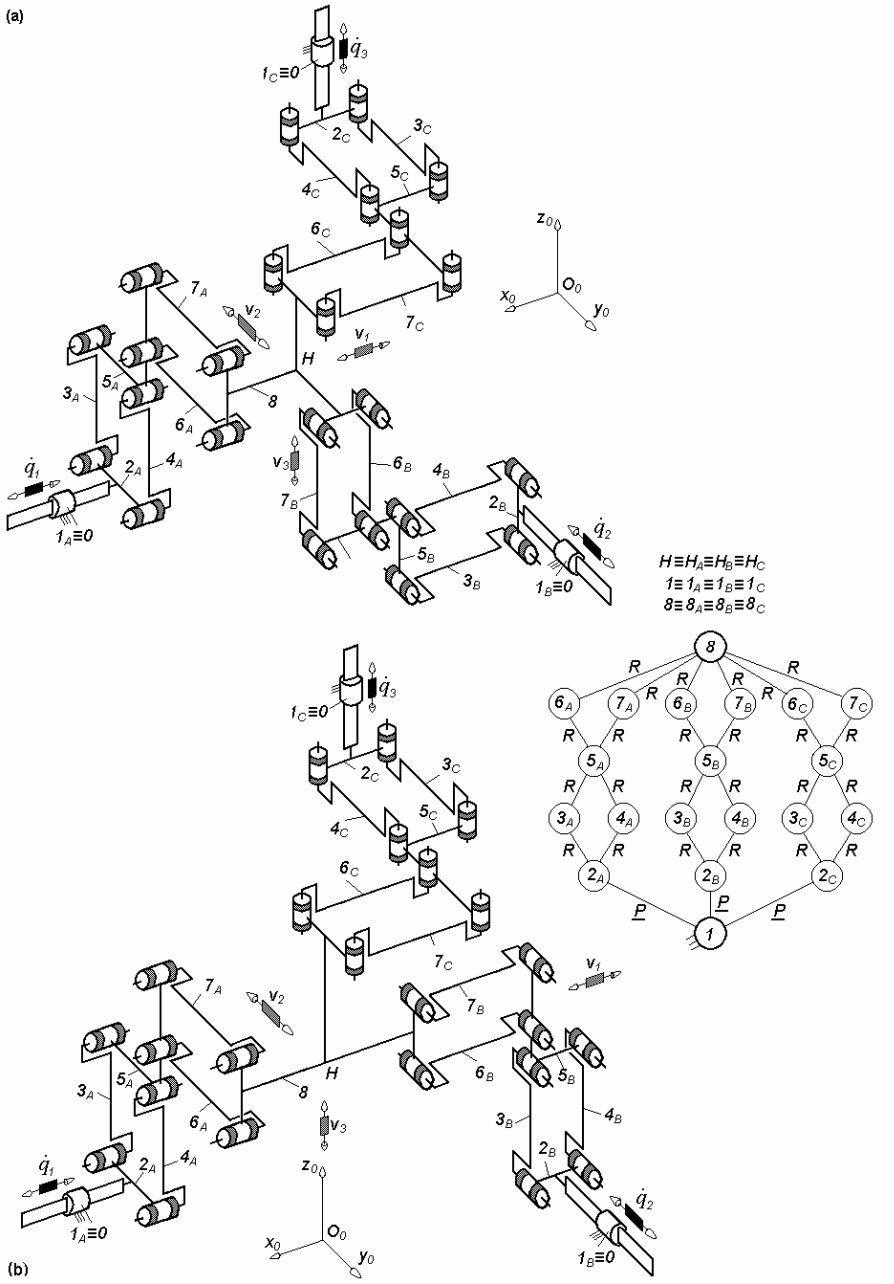

Fig. 7.8. *3-PPaPa*-type overconstrained maximally-regular TPMs defined by $M_F = S_F = 3$, $(R_F) = (\boldsymbol{v}_1, \boldsymbol{v}_2, \boldsymbol{v}_3)$, $T_F = 0$, $N_F = 24$, limb topology $\underline{P}||Pa||Pa$

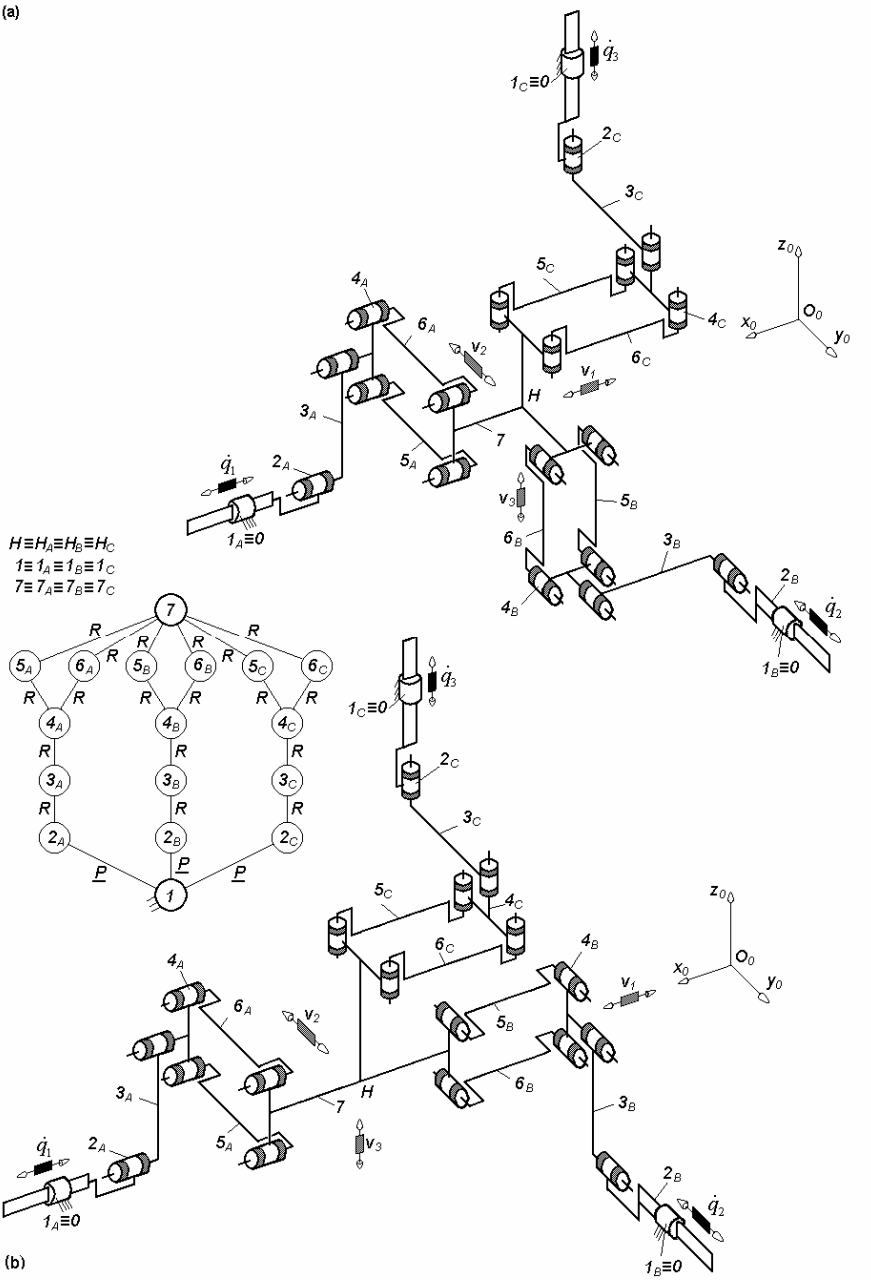

Fig. 7.9. *3-PRRPa*-type overconstrained maximally-regular TPMs defined by $M_F = S_F = 3$, $(R_F) = (\boldsymbol{v}_1, \boldsymbol{v}_2, \boldsymbol{v}_3)$, $T_F = 0$, $N_F = 12$, limb topology $\underline{P}||R||R||Pa$

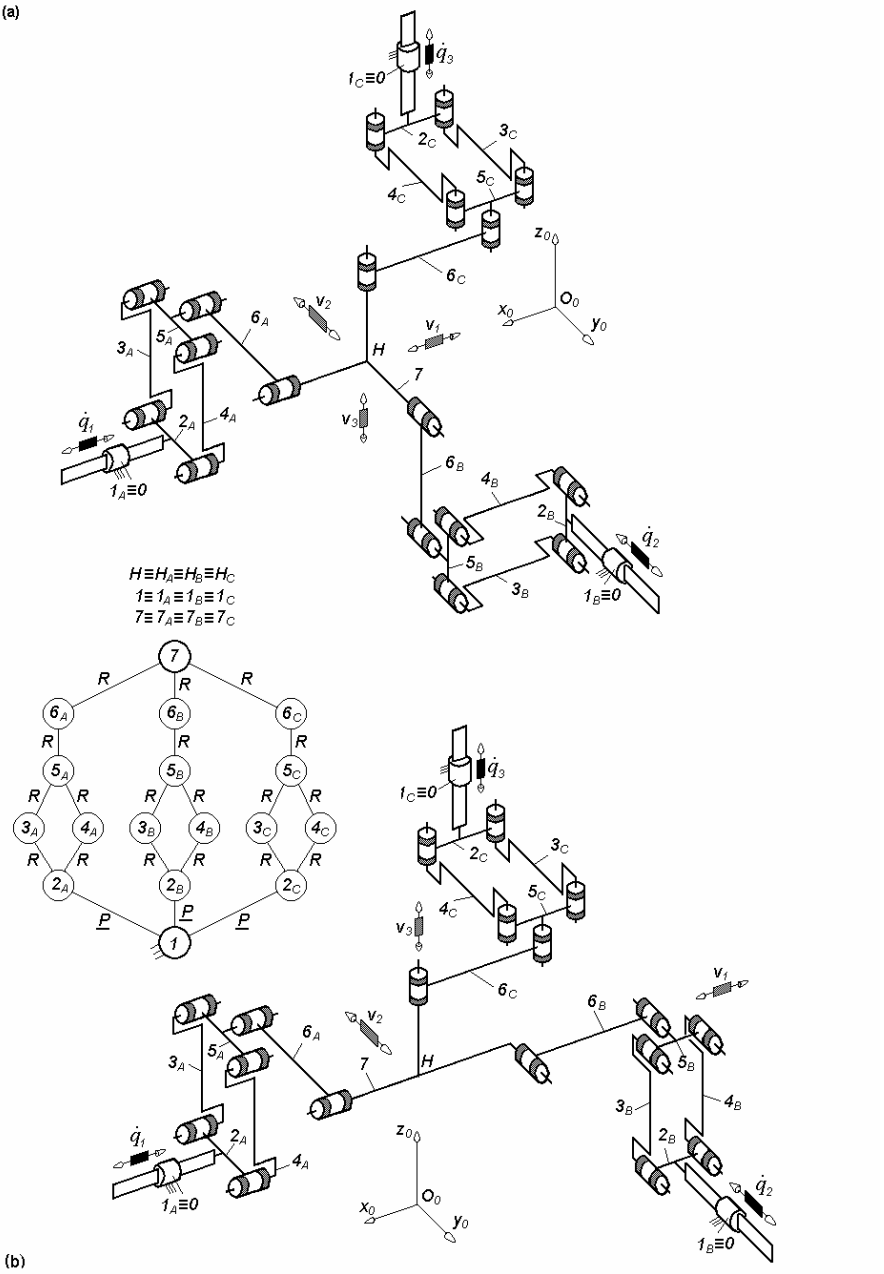

Fig. 7.10. *3-PPaRR*-type overconstrained maximally-regular TPMs defined by $M_F = S_F = 3$, $(R_F) = (\boldsymbol{v}_1, \boldsymbol{v}_2, \boldsymbol{v}_3)$, $T_F = 0$, $N_F = 12$, limb topology $\underline{P}||Pa||R||R$

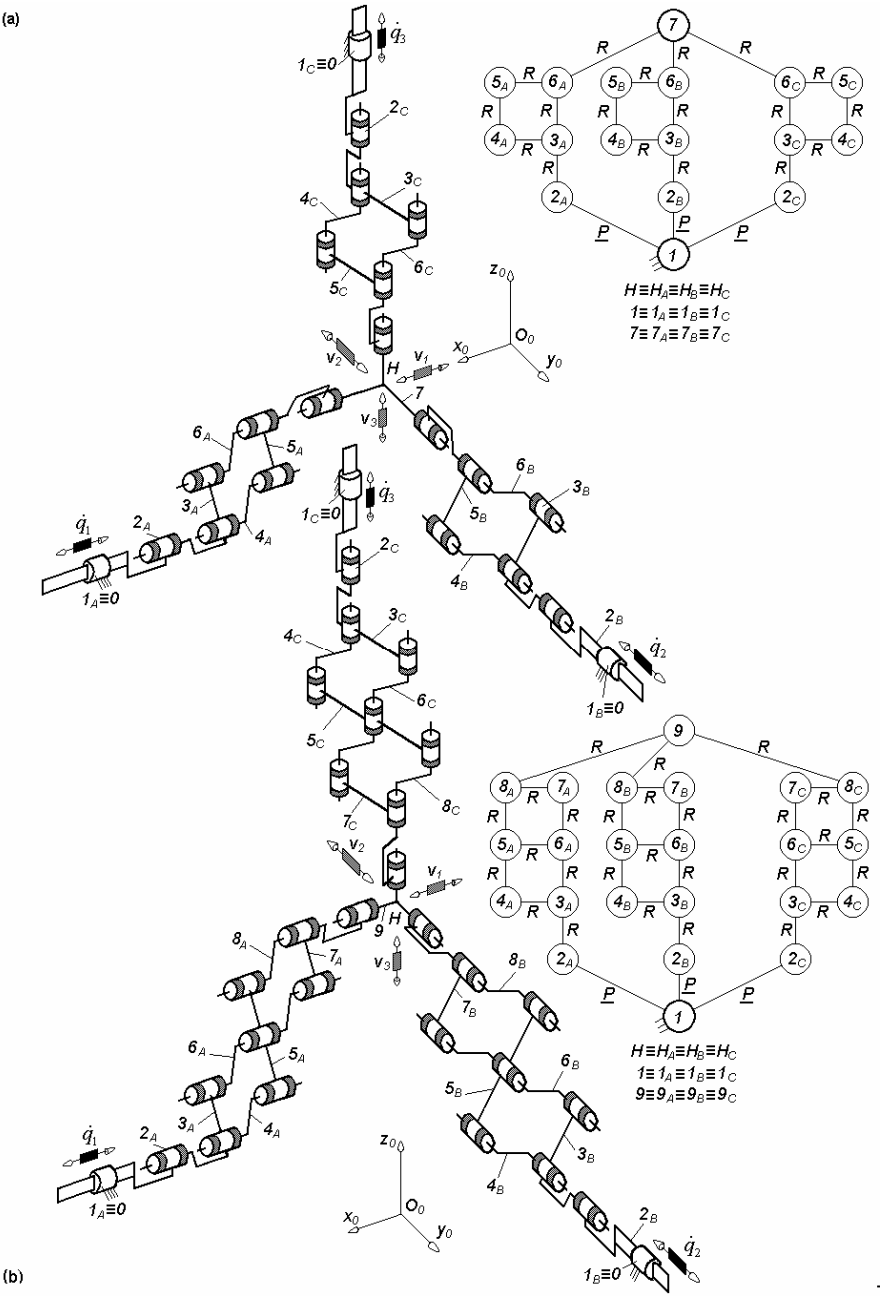

Fig. 7.11. Overconstrained maximally-regular TPMs of types *3-PRRbR* (**a**) and *3-PRRbRbR* (**b**) defined by $M_F = S_F = 3$, $(R_F) = (\boldsymbol{v}_1, \boldsymbol{v}_2, \boldsymbol{v}_3)$, $T_F = 0$, $N_F = 12$ (**a**), $N_F = 21$ (**b**), limb topology $\underline{P}||R||Rb||R$ (**a**) and $\underline{P}||R||Rb||Rb||R$ (**b**)

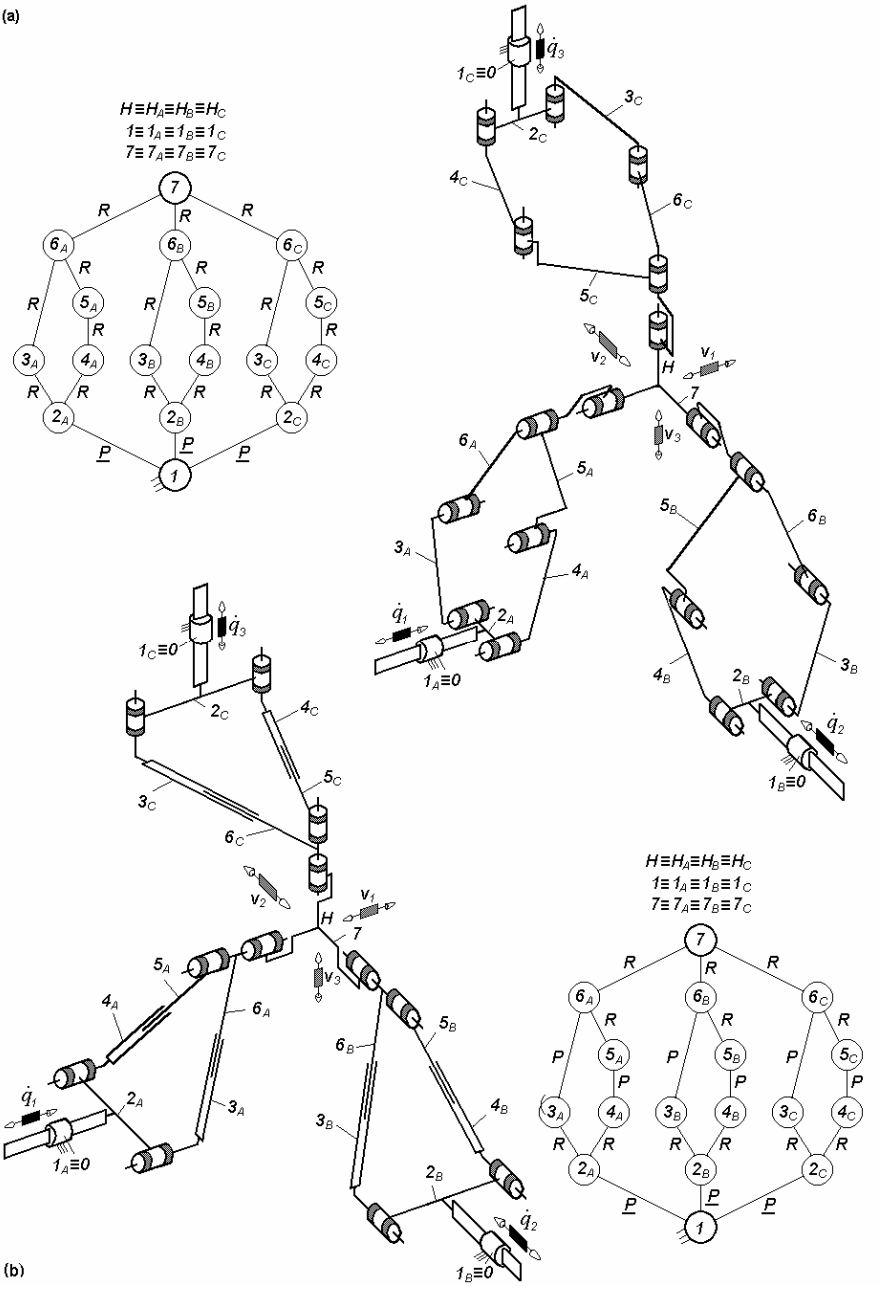

Fig. 7.12. *3-PPn2R*-type overconstrained maximally-regular TPMs defined by $M_F = S_F = 3$, $(R_F) = (\boldsymbol{v}_1, \boldsymbol{v}_2, \boldsymbol{v}_3)$, $T_F = 0$, $N_F = 12$, limb topology $\underline{P}||Pn2||R$

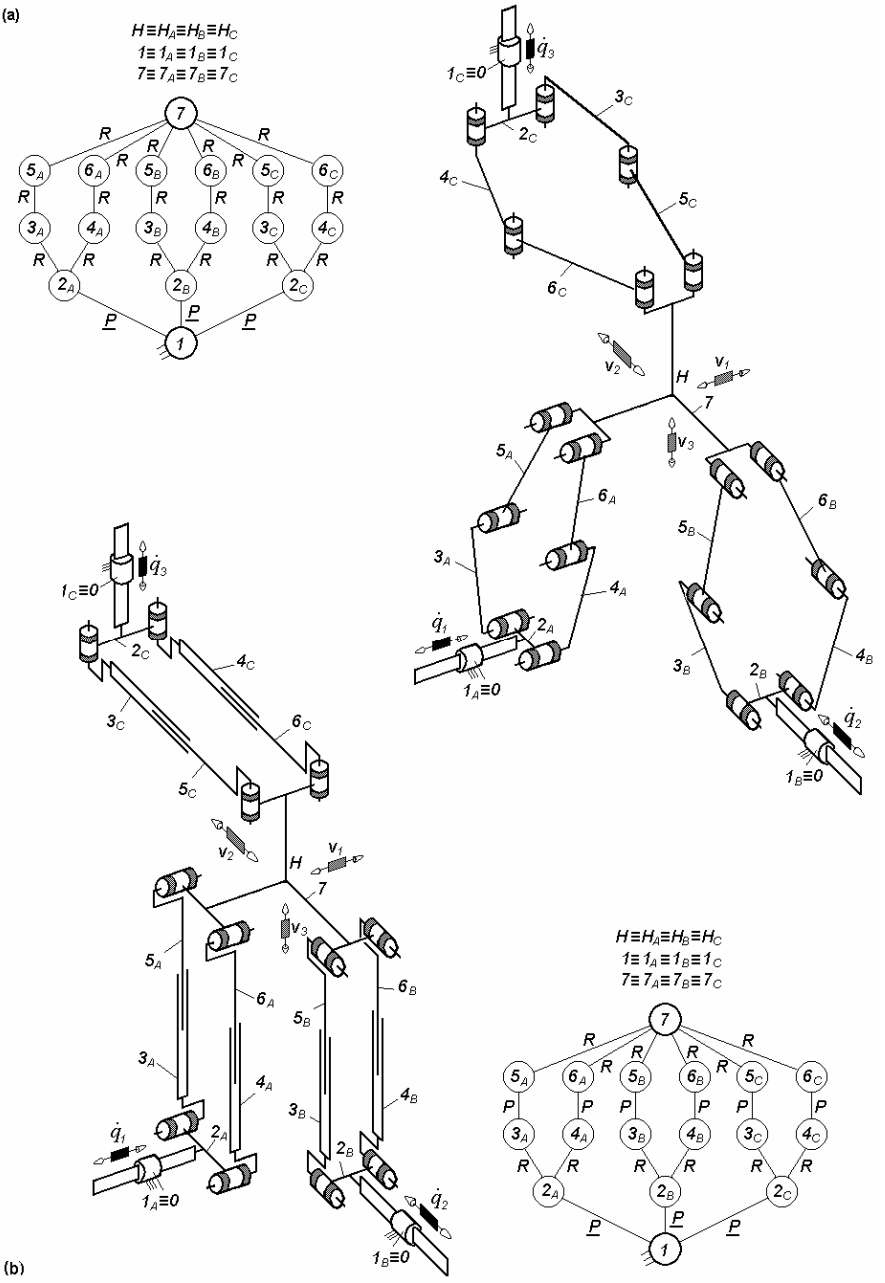

Fig. 7.13. *3-PPn3*-type overconstrained maximally-regular TPMs defined by $M_F = S_F = 3$, $(R_F) = (\boldsymbol{v}_1, \boldsymbol{v}_2, \boldsymbol{v}_3)$, $T_F = 0$, $N_F = 12$, limb topology $\underline{P}||Pn3$

7.1.2 Derived solutions with idle mobilities

Solutions with lower degrees of overconstraint can be derived from the basic solutions in Figs. 7.3–7.13 by using joints with *idle mobilities*. A large set of solutions can be obtained by introducing one or two rotational idle mobilities outside the closed loops that can be integrated in the limbs and up to three idle mobilities (two rotations and one translation) in each planar loop. The joints combining idle mobilities are denoted by an asterisk.

Examples of solutions with identical limbs and three to twelve degrees of overconstraint derived from the basic solutions in Figs. 7.3–7.13 are illustrated in Figs. 7.14–7.32. The limb topology and the number of overconstraints in these solutions are systematized in Table 7.5 and the structural parameters in Tables 7.4 and 7.6–7.9. We recall that two idle rotational mobilities are introduced in the spherical joint of the parallelogram loops denoted by Pa^{ccs} and Pa^{scc} which combine two cylindrical, one revolute and one spherical joint. In the cylindrical joint denoted by *C**, the rotation is an idle mobility. One idle translational mobility and two idle rotational mobilities are introduced in the prismatic and the spherical joints of each planar loop denoted by Pa^{cs}, Pb^{cs}, $Pn2^{cs}$ or $Pn3^{cs}$.

Table 7.4. Bases of the operational velocities spaces of the limbs isolated from the parallel mechanisms presented in Figs. 7.14–7.32

No.	Parallel mechanism	Basis (R_{G1})	(R_{G2})	(R_{G3})
1	Figs. 7.14a, 7.16a, 7.19a, 7.20a	$(\boldsymbol{v}_1,\boldsymbol{v}_2,\boldsymbol{v}_3,\boldsymbol{\omega}_\delta)$	$(\boldsymbol{v}_1,\boldsymbol{v}_2,\boldsymbol{v}_3,\boldsymbol{\omega}_\alpha)$	$(\boldsymbol{v}_1,\boldsymbol{v}_2,\boldsymbol{v}_3,\boldsymbol{\omega}_\beta)$
2	Fig. 7.14b	$(\boldsymbol{v}_1,\boldsymbol{v}_2,\boldsymbol{v}_3,\boldsymbol{\omega}_\beta)$	$(\boldsymbol{v}_1,\boldsymbol{v}_2,\boldsymbol{v}_3,\boldsymbol{\omega}_\alpha)$	$(\boldsymbol{v}_1,\boldsymbol{v}_2,\boldsymbol{v}_3,\boldsymbol{\omega}_\beta)$
3	Figs. 7.14c, 7.16b, 7.19b, 7.20b	$(\boldsymbol{v}_1,\boldsymbol{v}_2,\boldsymbol{v}_3,\boldsymbol{\omega}_\delta)$	$(\boldsymbol{v}_1,\boldsymbol{v}_2,\boldsymbol{v}_3,\boldsymbol{\omega}_\delta)$	$(\boldsymbol{v}_1,\boldsymbol{v}_2,\boldsymbol{v}_3,\boldsymbol{\omega}_\beta)$
4	Figs. 7.15a, 7.17a, 7.18a, 7.21a	$(\boldsymbol{v}_1,\boldsymbol{v}_2,\boldsymbol{v}_3,\boldsymbol{\omega}_\beta)$	$(\boldsymbol{v}_1,\boldsymbol{v}_2,\boldsymbol{v}_3,\boldsymbol{\omega}_\delta)$	$(\boldsymbol{v}_1,\boldsymbol{v}_2,\boldsymbol{v}_3,\boldsymbol{\omega}_\alpha)$
5	Fig. 7.15b	$(\boldsymbol{v}_1,\boldsymbol{v}_2,\boldsymbol{v}_3,\boldsymbol{\omega}_\delta)$	$(\boldsymbol{v}_1,\boldsymbol{v}_2,\boldsymbol{v}_3,\boldsymbol{\omega}_\delta)$	$(\boldsymbol{v}_1,\boldsymbol{v}_2,\boldsymbol{v}_3,\boldsymbol{\omega}_\alpha)$
6	Figs. 7.15c, 7.17b, 7.18b, 7.21b	$(\boldsymbol{v}_1,\boldsymbol{v}_2,\boldsymbol{v}_3,\boldsymbol{\omega}_\beta)$	$(\boldsymbol{v}_1,\boldsymbol{v}_2,\boldsymbol{v}_3,\boldsymbol{\omega}_\alpha)$	$(\boldsymbol{v}_1,\boldsymbol{v}_2,\boldsymbol{v}_3,\boldsymbol{\omega}_\alpha)$
7	Figs. 7.22, 7.24, 7.26b, 7.27, 7.29a, 7.30a, 7.31	$(\boldsymbol{v}_1,\boldsymbol{v}_2,\boldsymbol{v}_3,\boldsymbol{\omega}_\alpha,\boldsymbol{\omega}_\beta)$	$(\boldsymbol{v}_1,\boldsymbol{v}_2,\boldsymbol{v}_3,\boldsymbol{\omega}_\beta,\boldsymbol{\omega}_\delta)$	$(\boldsymbol{v}_1,\boldsymbol{v}_2,\boldsymbol{v}_3,\boldsymbol{\omega}_\alpha,\boldsymbol{\omega}_\delta)$
8	Figs. 7.23, 7.25, 7.26b, 7.28, .471b, 7.30b, 7.32	$(\boldsymbol{v}_1,\boldsymbol{v}_2,\boldsymbol{v}_3,\boldsymbol{\omega}_\alpha)$	$(\boldsymbol{v}_1,\boldsymbol{v}_2,\boldsymbol{v}_3,\boldsymbol{\omega}_\beta)$	$(\boldsymbol{v}_1,\boldsymbol{v}_2,\boldsymbol{v}_3,\boldsymbol{\omega}_\delta)$

Table 7.5. Limb topology and the number of overconstraints N_F in the derived maximally regular TPMs presented in Figs. 7.14–7.32

No.	Basic TPM type	N_F	Derived TPM type	N_F	Limb topology
1	*3-$\underline{P}$PP* (Fig. 7.3)	*6*	*3-$\underline{P}$PC** (Fig. 7.14)	*3*	$\underline{P} \perp P \perp^{\perp} C^*$
2			*3-$\underline{P}$C*P* (Fig. 7.15)	*3*	$\underline{P} \perp C^* \perp^{\perp} P$
3	*3-$\underline{P}$PaP* (Fig. 7.6)	*15*	*3-$\underline{P}$PaC** (Fig. 7.16)	*12*	$\underline{P}\|\|Pa \perp C^*$
4			*3-$\underline{P}$Pa^{ss}P* (Fig. 7.17)	*3*	$\underline{P}\|\|Pa^{ss} \perp P$
5	*3-$\underline{P}$PPa* (Fig. 7.7)	*15*	*3-$\underline{P}$C*Pa* (Fig. 7.18)	*12*	$\underline{P} \perp C^* \perp^{\|\|} Pa$
6			*3-$\underline{P}$PPa^{ss}* (Fig. 7.19)	*3*	$\underline{P} \perp P \perp^{\|\|} Pa^{ss}$
7	*3-$\underline{P}$PaPa* (Fig. 7.8)	*24*	*3-$\underline{P}$PaPa^{ss}* (Fig. 7.20)	*12*	$\underline{P}\|\|Pa\|\|Pa^{ss}$
8			*3-$\underline{P}$Pa^{ss}Pa* (Fig. 7.21)	*12*	$\underline{P}\|\|Pa^{ss}\|\|Pa$
9	*3-$\underline{P}$RRPa* (Fig. 7.9)	*12*	*3-$\underline{P}$R*RRPa* (Fig. 7.22)	*9*	$\underline{P} \perp R^* \perp^{\|\|} R\|\|R\|\|Pa$
10			*3-$\underline{P}$RRPa^{cs}* (Fig. 7.23)	*3*	$\underline{P}\|\|R\|\|R\|\|Pa^{cs}$
11	*3-$\underline{P}$PaRR* (Fig. 7.10)	*12*	*3-$\underline{P}$PaRRR** (Fig. 7.24)	*9*	$\underline{P}\|\|Pa\|\|R\|\|R \perp R^*$
12			*3-$\underline{P}$Pa^{cs}RR* (Fig. 7.25)	*3*	$\underline{P}\|\|Pa^{cs}\|\|R\|\|R$
13	*3-$\underline{P}$RRbR* (Fig. 7.11a)	*12*	*3-$\underline{P}$R*RRbR* (Fig. 7.26a)	*9*	$\underline{P} \perp R^* \perp^{\|\|} R\|\|Rb\|\|R$
14			*3-$\underline{P}$RRb^{cs}R* (Fig. 7.26b)	*3*	$\underline{P}\|\|R\|\|Rb^{cs}\|\|R$
15	*3-$\underline{P}$RRbRbR* (Fig. 7.11b)	*21*	*3-$\underline{P}$R*RRbRbR* (Fig. 7.27)	*18*	$\underline{P} \perp R^* \perp^{\|\|} R\|\|Rb\|\|Rb\|\|R$
16			*3-$\underline{P}$RRb^{cs}Rb^{cs}R* (Fig. 7.28)	*3*	$\underline{P}\|\|R\|\|Rb^{cs}\|\|Rb^{cs}\|\|R$
17	*3-$\underline{P}$Pn2R* (Fig. 7.12a, b)	*12*	*3-$\underline{P}$Pn2RR** (Figs. 7.29a, 7.30a)	*9*	$\underline{P}\|\|Pn2\|\|R \perp R^*$
18			*3-$\underline{P}$Pn2^{cs}R* (Figs. 7.29b, 7.30b)	*3*	$\underline{P}\|\|Pn2^{cs}\|\|R$
19	*3-$\underline{P}$Pn3* (Fig. 7.13a, b)	*12*	*3-$\underline{P}$Pn3R** (Fig. 7.31a, b)	*9*	$\underline{P}\|\|Pn3 \perp R^*$
20			*3-$\underline{P}$Pn3^{cs}* (Fig. 7.32a, b)	*3*	$\underline{P}\|\|Pn3^{cs}$

Table 7.6. Structural parameters[a] of translational parallel mechanisms in Figs. 7.14–7.19

No.	Structural parameter	Solution *3-PPC** (Fig. 7.14) *3-PC*P* (Fig. 7.15)	*3-PPaC** (Fig. 7.16) *3-PC*Pa* (Fig. 7.18)	*3-PPa^{ss}P* (Fig. 7.17) *3-PPPa^{ss}* (Fig. 7.19)
1	m	8	14	14
2	p_1	3	6	6
3	p_2	3	6	6
4	p_3	3	6	6
5	p	9	18	18
6	q	2	5	5
7	k_1	3	0	0
8	k_2	0	3	3
9	k	3	3	3
10	(R_{Gi}) $(i = 1,2,3)$	See Table 7.4	See Table 7.4	See Table 7.4
11	S_{G1}	4	4	4
12	S_{G2}	4	4	4
13	S_{G3}	4	4	4
14	r_{G1}	0	3	6
15	r_{G2}	0	3	6
16	r_{G3}	0	3	6
17	M_{G1}	4	4	4
18	M_{G2}	4	4	4
19	M_{G3}	4	4	4
20	(R_F)	$(\boldsymbol{v}_1, \boldsymbol{v}_2, \boldsymbol{v}_3)$	$(\boldsymbol{v}_1, \boldsymbol{v}_2, \boldsymbol{v}_3)$	$(\boldsymbol{v}_1, \boldsymbol{v}_2, \boldsymbol{v}_3)$
21	S_F	3	3	3
22	r_1	0	9	18
23	r_F	9	18	27
24	M_F	3	3	3
25	N_F	3	12	3
26	T_F	0	0	0
27	$\sum_{j=1}^{p_1} f_j$	4	7	10
28	$\sum_{j=1}^{p_2} f_j$	4	7	10
29	$\sum_{j=1}^{p_3} f_j$	4	7	10
30	$\sum_{j=1}^{p} f_j$	12	21	30

[a]See footnote of Table 2.1 for the nomenclature of structural parameters

Table 7.7. Structural parameters[a] of translational parallel mechanisms in Figs. 7.20–7.26

No.	Structural parameter	Solution *3-PPaPa^{ss}* (Fig. 7.20) *3-PPa^{ss}Pa* (Fig. 7.21)	*3-PR*RRPa* (Fig. 7.22) *3-PPaRRR** (Fig. 7.24) *3-PR*RRbR* (Fig. 7.26a)	*3-PRRPa^{cs}* (Fig. 7.23) *3-PPa^{cs}RR* (Fig. 7.25) *3-PRRb^{cs}R* (Fig. 7.26b)
1	m	20	20	17
2	p_1	9	8	7
3	p_2	9	8	7
4	p_3	9	8	7
5	p	27	24	21
6	q	8	5	5
7	k_1	0	0	0
8	k_2	3	3	3
9	k	3	3	3
10	(R_{Gi}) $(i = 1,2,3)$	See Table 7.4	See Table 7.4	See Table 7.4
11	S_{G1}	4	5	4
12	S_{G2}	4	5	4
13	S_{G3}	4	5	4
14	r_{G1}	9	3	6
15	r_{G2}	9	3	6
16	r_{G3}	9	3	6
17	M_{G1}	4	5	4
18	M_{G2}	4	5	4
19	M_{G3}	4	5	4
20	(R_F)	$(\boldsymbol{v}_1, \boldsymbol{v}_2, \boldsymbol{v}_3)$	$(\boldsymbol{v}_1, \boldsymbol{v}_2, \boldsymbol{v}_3)$	$(\boldsymbol{v}_1, \boldsymbol{v}_2, \boldsymbol{v}_3)$
21	S_F	3	3	3
22	r_1	27	9	18
23	r_F	36	21	27
24	M_F	3	3	3
25	N_F	12	9	3
26	T_F	0	0	0
27	$\sum_{j=1}^{p_1} f_j$	13	8	10
28	$\sum_{j=1}^{p_2} f_j$	13	8	10
29	$\sum_{j=1}^{p_3} f_j$	13	8	10
30	$\sum_{j=1}^{p} f_j$	39	24	30

[a]See footnote of Table 2.1 for the nomenclature of structural parameters

Table 7.8. Structural parameters[a] of translational parallel mechanisms in Figs. 7.27 and 7.28

No.	Structural parameter	Solution *3-PR*RRbRbR* (Fig. 7.27)	*3-PRRb^{cs}Rb^{cs}R* (Fig. 7.28)
1	m	26	23
2	p_1	11	10
3	p_2	11	10
4	p_3	11	10
5	p	33	30
6	q	8	8
7	k_1	0	0
8	k_2	3	3
9	k	3	3
10	(R_{Gi}) (i = *1,2,3*)	See Table 7.4	See Table 7.4
11	S_{G1}	5	4
12	S_{G2}	5	4
13	S_{G3}	5	4
14	r_{G1}	6	12
15	r_{G2}	6	12
16	r_{G3}	6	12
17	M_{G1}	5	4
18	M_{G2}	5	4
19	M_{G3}	5	4
20	(R_F)	($\boldsymbol{v}_1,\boldsymbol{v}_2,\boldsymbol{v}_3$)	($\boldsymbol{v}_1,\boldsymbol{v}_2,\boldsymbol{v}_3$)
21	S_F	3	3
22	r_1	18	36
23	r_F	30	45
24	M_F	3	3
25	N_F	18	3
26	T_F	0	0
27	$\sum_{j=1}^{p_1} f_j$	11	16
28	$\sum_{j=1}^{p_2} f_j$	11	16
29	$\sum_{j=1}^{p_3} f_j$	11	16
30	$\sum_{j=1}^{p} f_j$	33	48

[a]See footnote of Table 2.1 for the nomenclature of structural parameters

Table 7.9. Structural parameters[a] of translational parallel mechanisms in Figs. 7.29–7.32

No.	Structural parameter	Solution *3-PPn2RR** (Figs. 7.29a, 7.30a) *3-PPn3R** (Fig. 7.31a, b)	 *3-PPn2^{cs}R* (Figs. 7.29b, 7.30b) *3-PPn3^{cs}* (Fig. 7.32a, b)
1	m	20	17
2	p_1	8	7
3	p_2	8	7
4	p_3	8	7
5	p	24	21
6	q	5	5
7	k_1	0	0
8	k_2	3	3
9	k	3	3
10	(R_{Gi}) $(i = 1,2,3)$	See Table 7.4	See Table 7.4
11	S_{G1}	5	4
12	S_{G2}	5	4
13	S_{G3}	5	4
14	r_{G1}	3	6
15	r_{G2}	3	6
16	r_{G3}	3	6
17	M_{G1}	5	4
18	M_{G2}	5	4
19	M_{G3}	5	4
20	(R_F)	$(\boldsymbol{v}_1, \boldsymbol{v}_2, \boldsymbol{v}_3)$	$(\boldsymbol{v}_1, \boldsymbol{v}_2, \boldsymbol{v}_3)$
21	S_F	3	3
22	r_1	9	18
23	r_F	21	27
24	M_F	3	3
25	N_F	9	3
26	T_F	0	0
27	$\sum_{j=1}^{p_1} f_j$	8	10
28	$\sum_{j=1}^{p_2} f_j$	8	10
29	$\sum_{j=1}^{p_3} f_j$	8	10
30	$\sum_{j=1}^{p} f_j$	24	30

[a]See footnote of Table 2.1 for the nomenclature of structural parameters

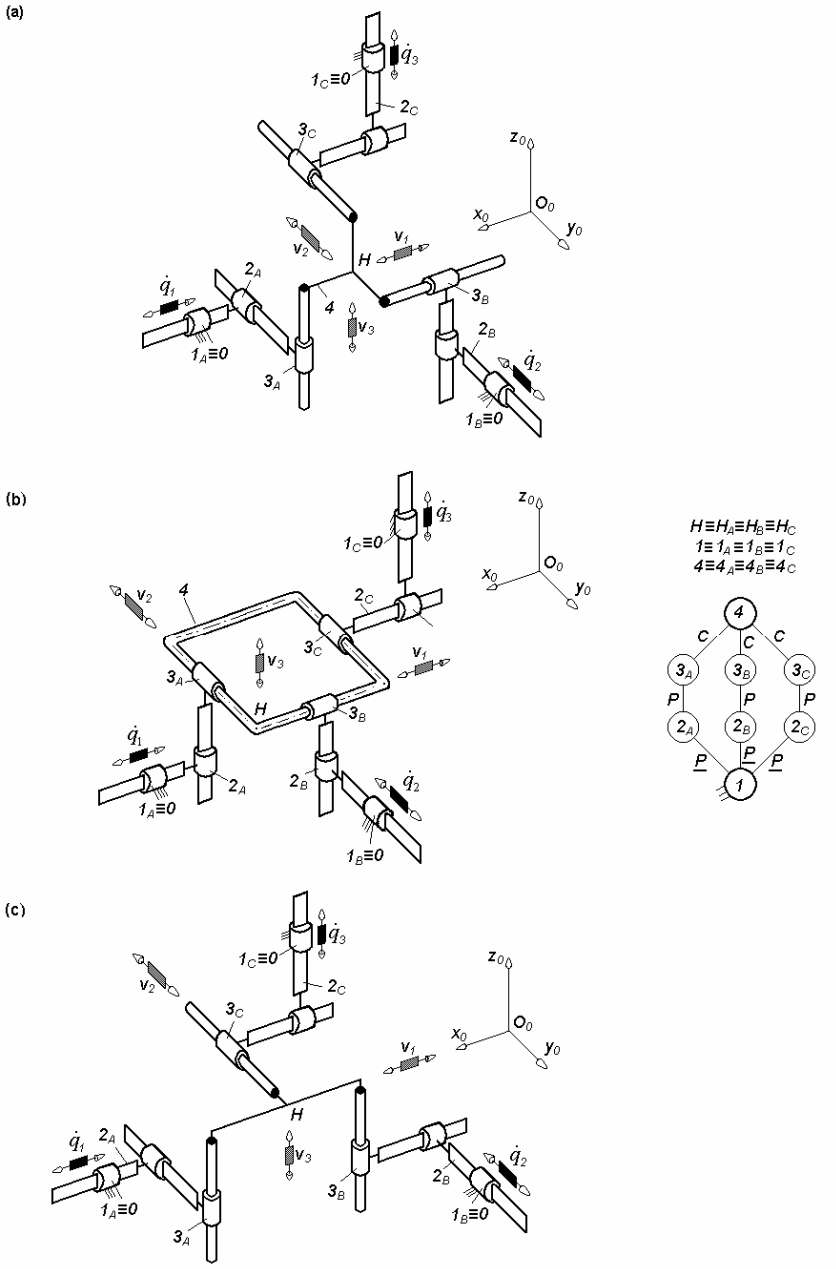

Fig. 7.14. *3-PPC**-type overconstrained maximally-regular TPMs defined by $M_F = S_F = 3$, $(R_F) = (\boldsymbol{v}_1, \boldsymbol{v}_2, \boldsymbol{v}_3)$, $T_F = 0$, $N_F = 3$, limb topology $\underline{P} \perp P \perp^{\perp} C^*$

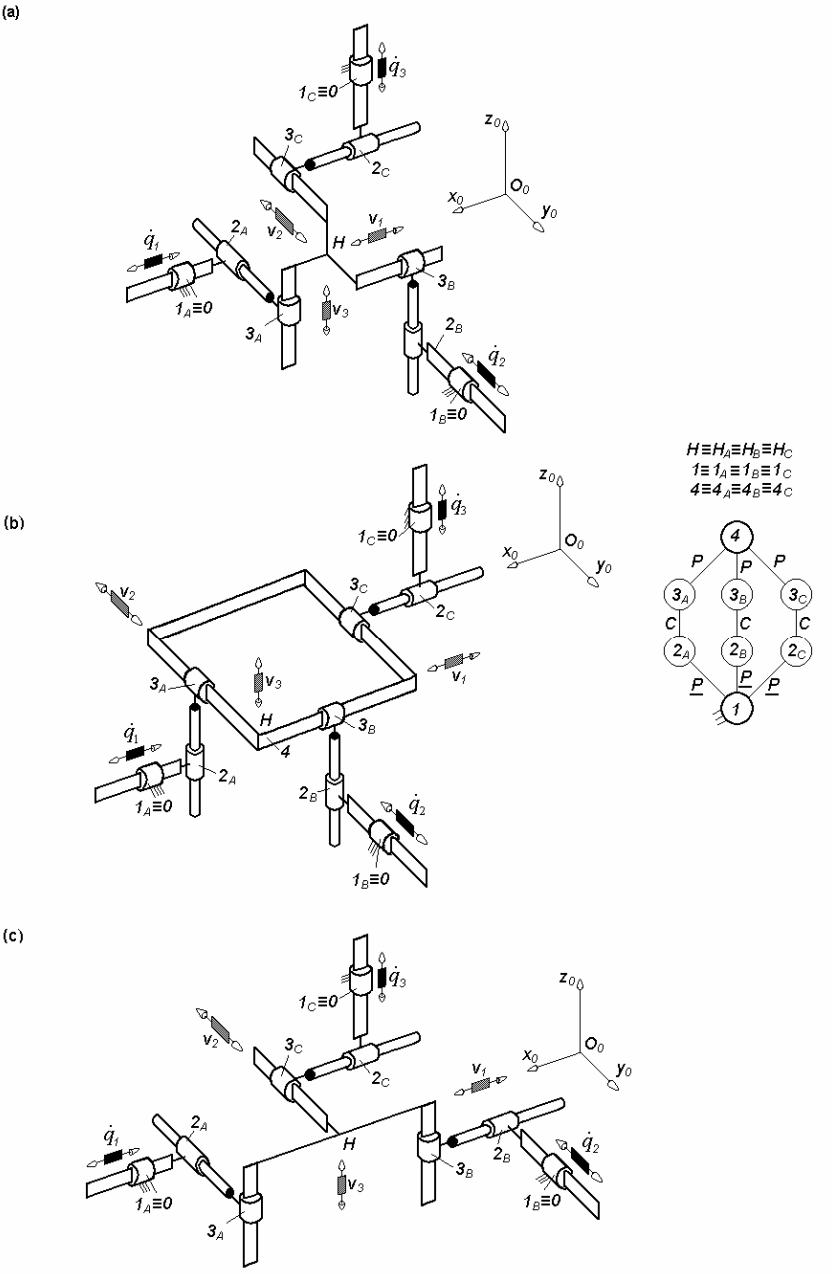

Fig. 7.15. *3-PC*P*-type overconstrained maximally-regular TPMs defined by $M_F = S_F = 3$, $(R_F) = (\boldsymbol{v}_1, \boldsymbol{v}_2, \boldsymbol{v}_3)$, $T_F = 0$, $N_F = 3$, limb topology $\underline{P} \perp C^* \perp^{\perp} P$

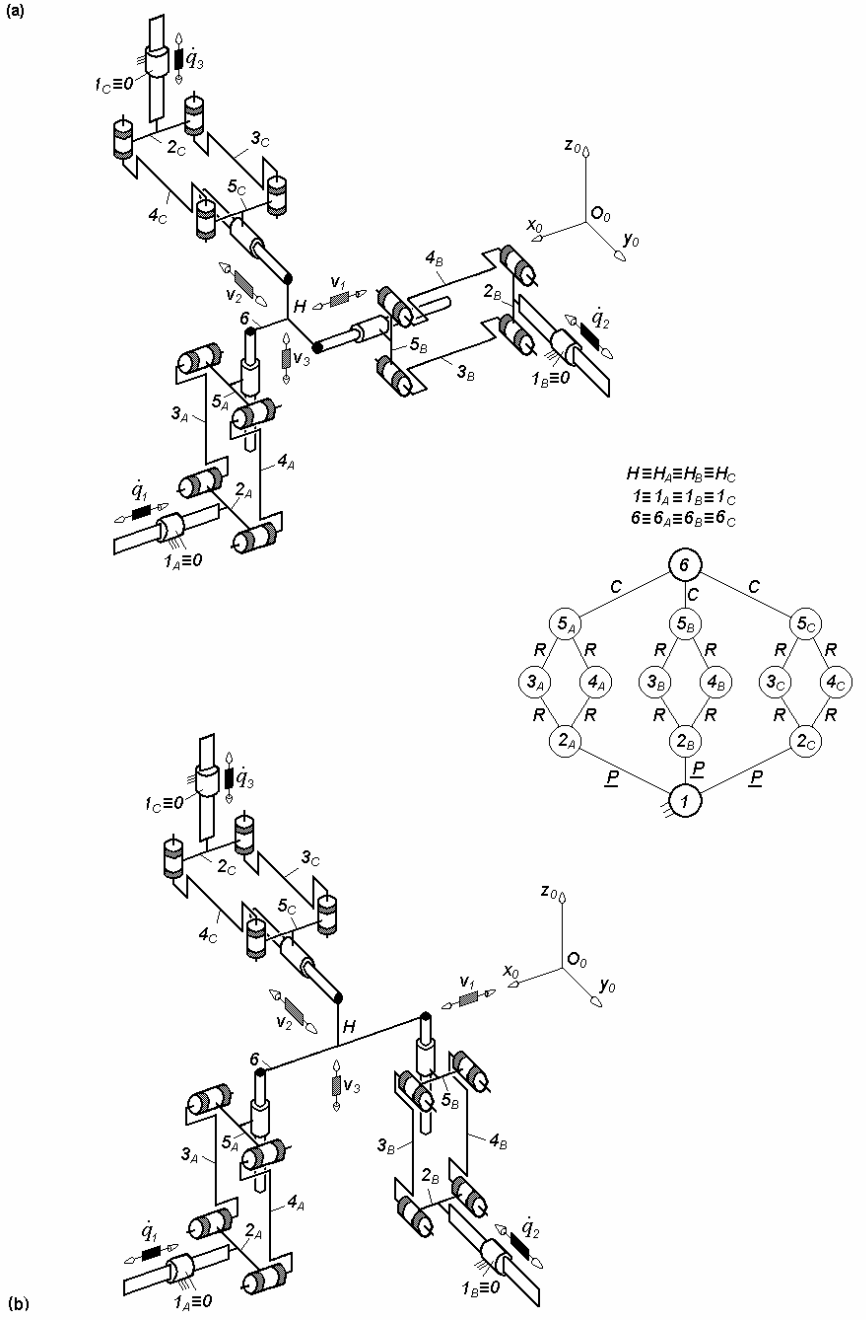

Fig. 7.16. *3-PPaC**-type overconstrained maximally-regular TPMs defined by $M_F = S_F = 3$, $(R_F) = (\boldsymbol{v}_1, \boldsymbol{v}_2, \boldsymbol{v}_3)$, $T_F = 0$, $N_F = 12$, limb topology $\underline{P}||Pa \perp C^*$

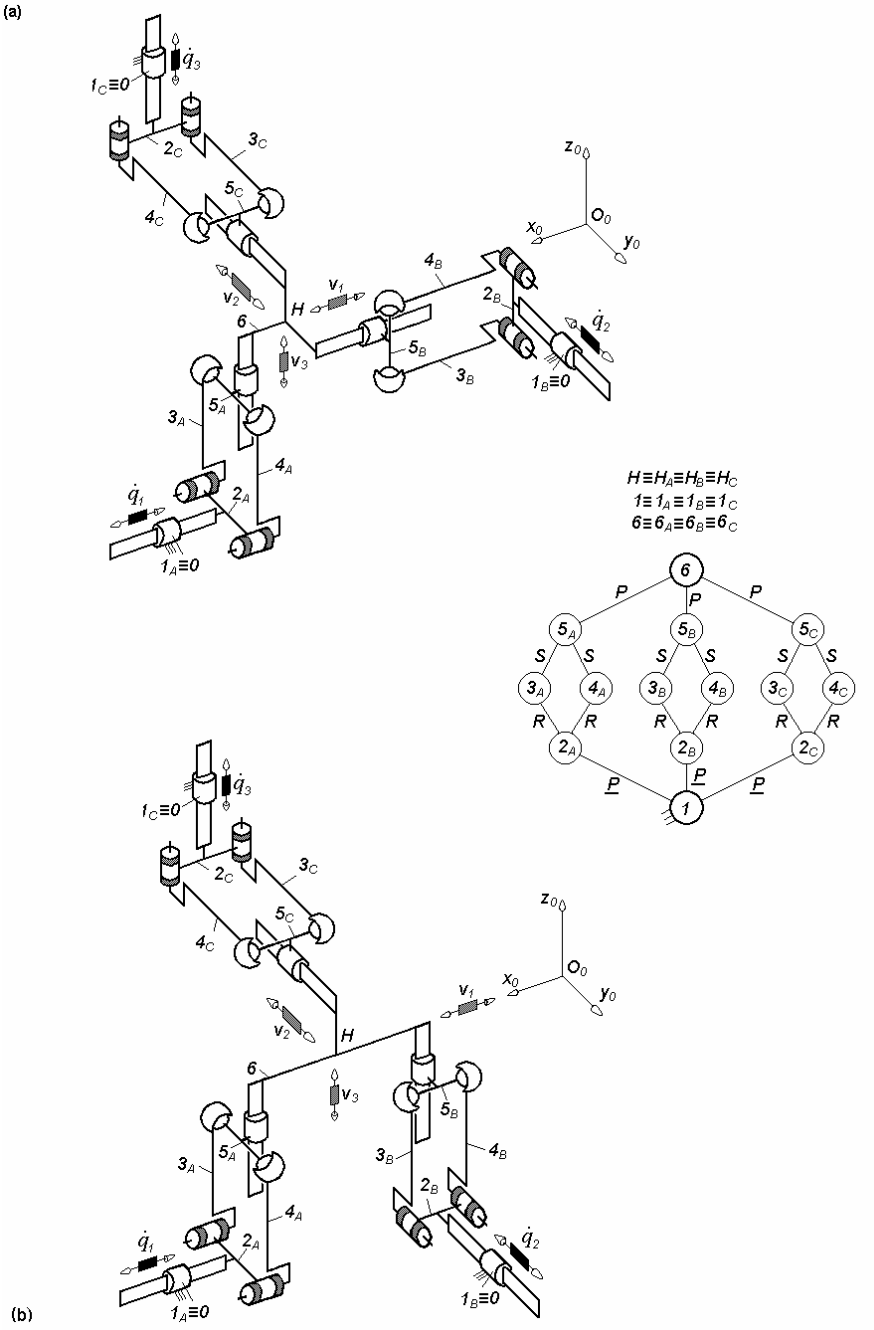

Fig. 7.17. *3-*$\underline{P}$*P*a^{ss}*P*-type overconstrained maximally-regular TPMs defined by $M_F = S_F = 3$, $(R_F) = (\boldsymbol{v}_1, \boldsymbol{v}_2, \boldsymbol{v}_3)$, $T_F = 0$, $N_F = 3$, limb topology $\underline{P}||Pa^{ss} \perp P$

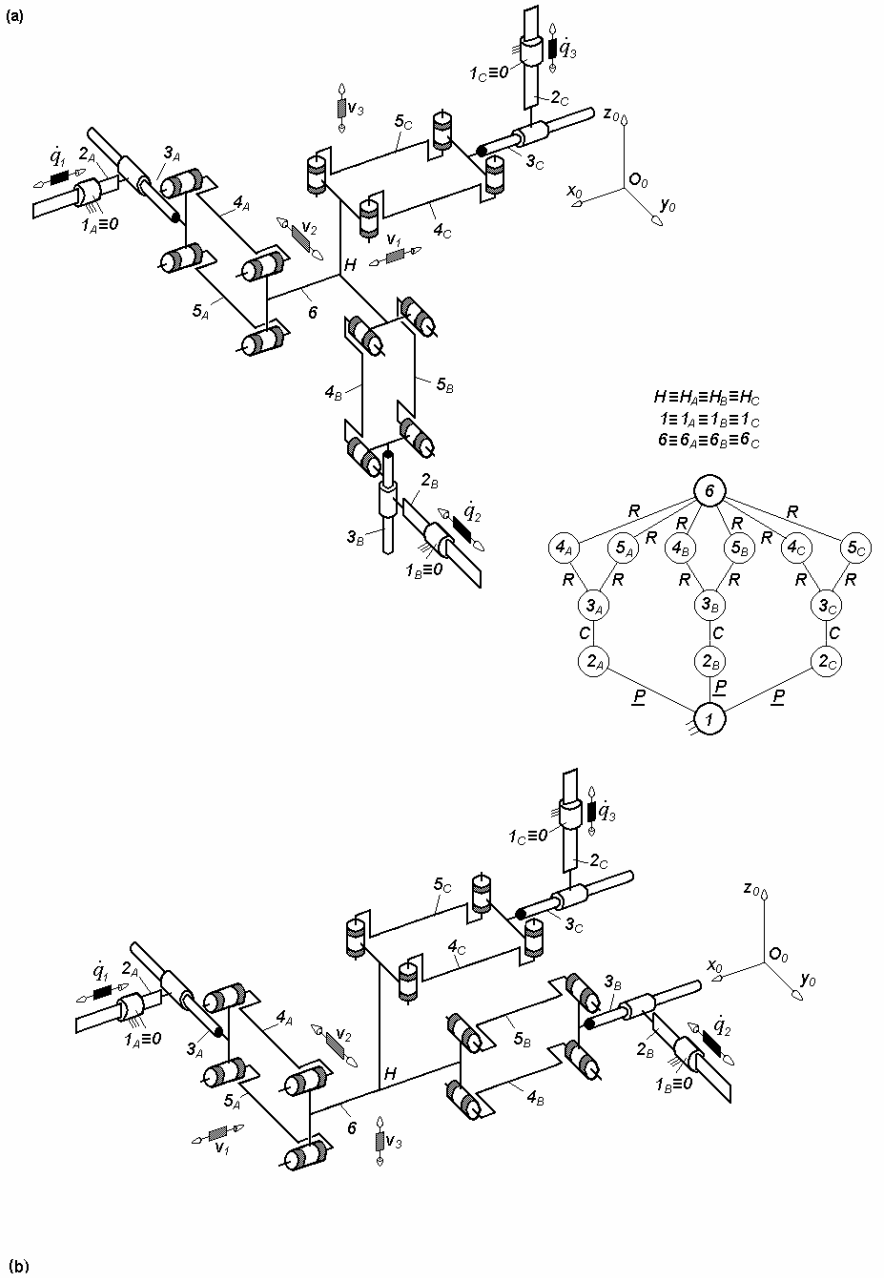

Fig. 7.18. *3-PC*Pa*-type overconstrained maximally-regular TPMs defined by $M_F = S_F = 3$, $(R_F) = (\boldsymbol{v}_1, \boldsymbol{v}_2, \boldsymbol{v}_3)$, $T_F = 0$, $N_F = 12$, limb topology $\underline{P} \perp C^* \perp \| Pa$

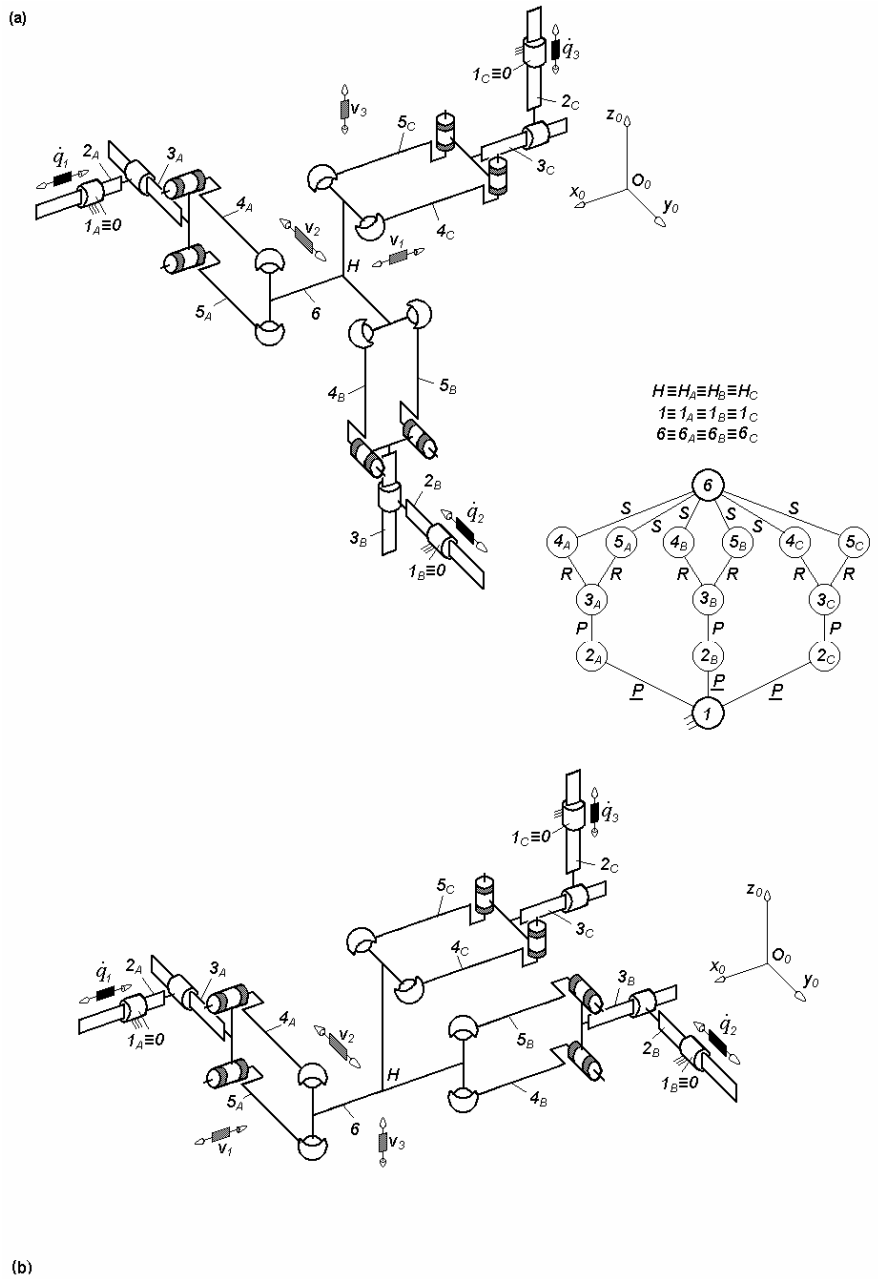

Fig. 7.19. *3-*$\underline{P}PPa^{ss}$-type overconstrained maximally-regular TPMs defined by $M_F = S_F = 3$, $(R_F) = (\boldsymbol{v}_1, \boldsymbol{v}_2, \boldsymbol{v}_3)$, $T_F = 0$, $N_F = 3$, limb topology $\underline{P} \perp P \perp {}^{\parallel}Pa^{ss}$

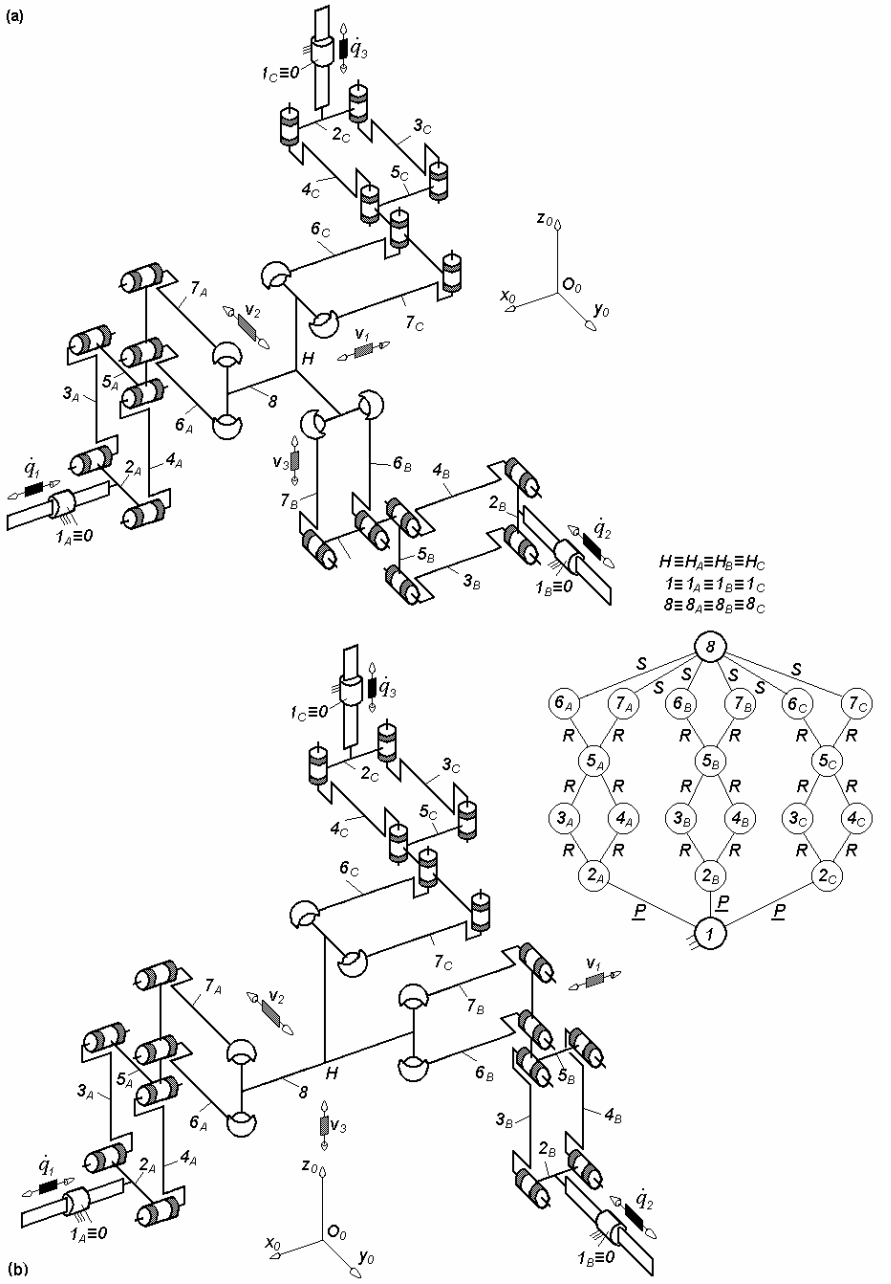

Fig. 7.20. *3-*$\underline{P}$*PaPa*^{ss}-type overconstrained maximally-regular TPMs defined by $M_F = S_F = 3$, $(R_F) = (\boldsymbol{v}_1, \boldsymbol{v}_2, \boldsymbol{v}_3)$, $T_F = 0$, $N_F = 12$, limb topology $\underline{P}||Pa||Pa^{ss}$

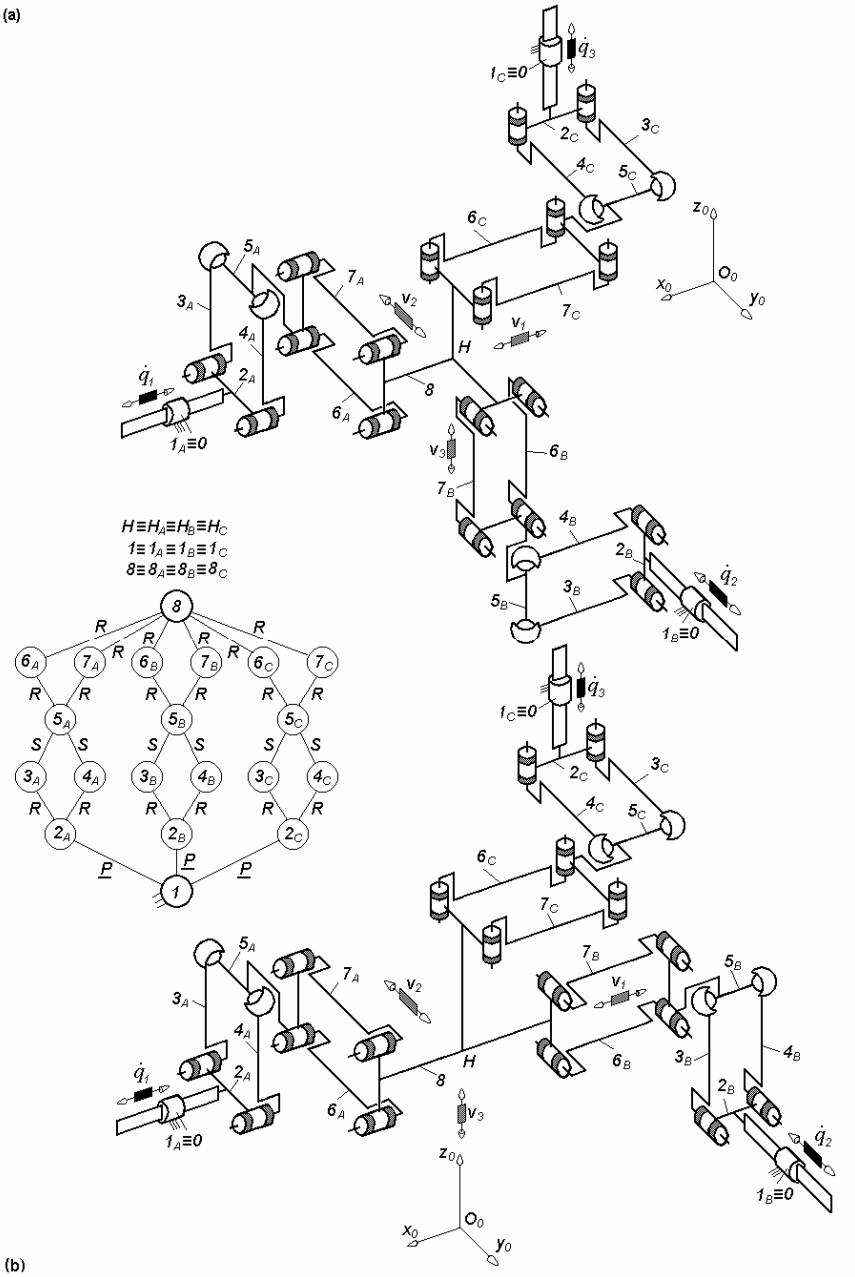

Fig. 7.21. *3-$\underline{P}Pa^{ss}Pa$*-type overconstrained maximally-regular TPMs defined by $M_F = S_F = 3$, $(R_F) = (\boldsymbol{v}_1, \boldsymbol{v}_2, \boldsymbol{v}_3)$, $T_F = 0$, $N_F = 12$, limb topology $\underline{P}||Pa^{ss}||Pa$

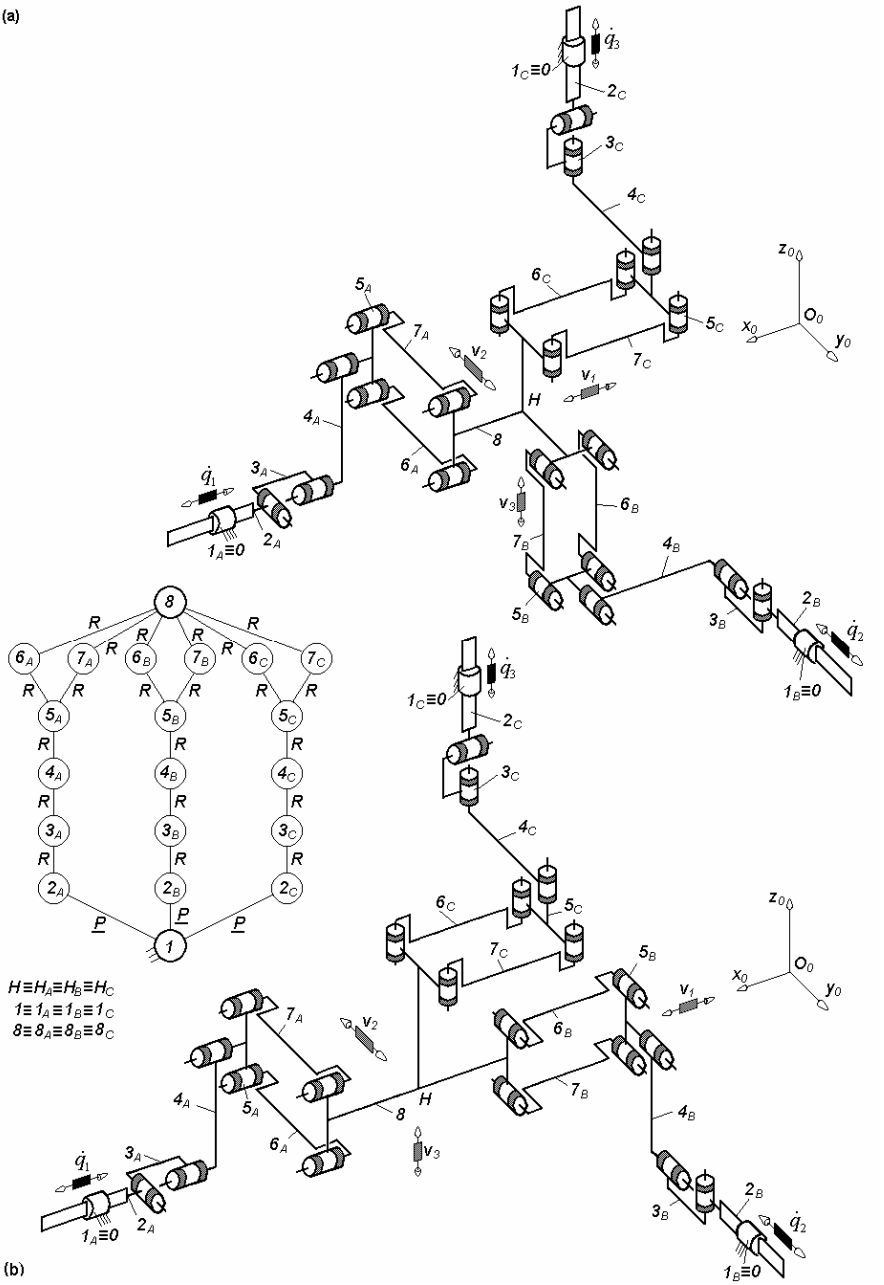

Fig. 7.22. *3-PR*RRPa*-type overconstrained maximally-regular TPMs defined by $M_F = S_F = 3$, $(R_F) = (\boldsymbol{v}_1, \boldsymbol{v}_2, \boldsymbol{v}_3)$, $T_F = 0$, $N_F = 9$, limb topology $\underline{P} \perp R^* \perp {}^{\parallel}R||R||Pa$

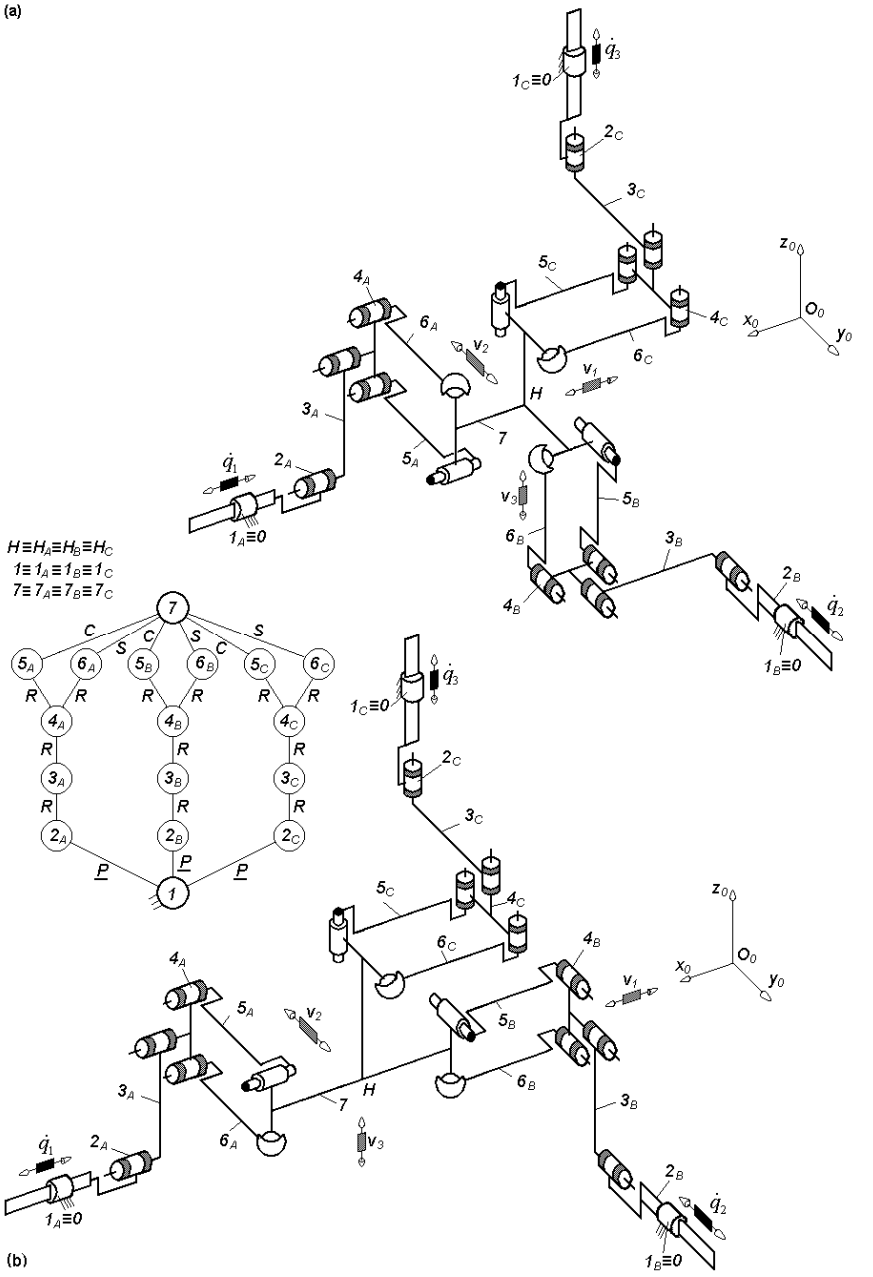

Fig. 7.23. *3-<u>P</u>RRPa^{cs}*-type overconstrained maximally-regular TPMs defined by $M_F = S_F = 3$, $(R_F) = (\boldsymbol{v}_1, \boldsymbol{v}_2, \boldsymbol{v}_3)$, $T_F = 0$, $N_F = 3$, limb topology $\underline{P}||R||R||Pa^{cs}$

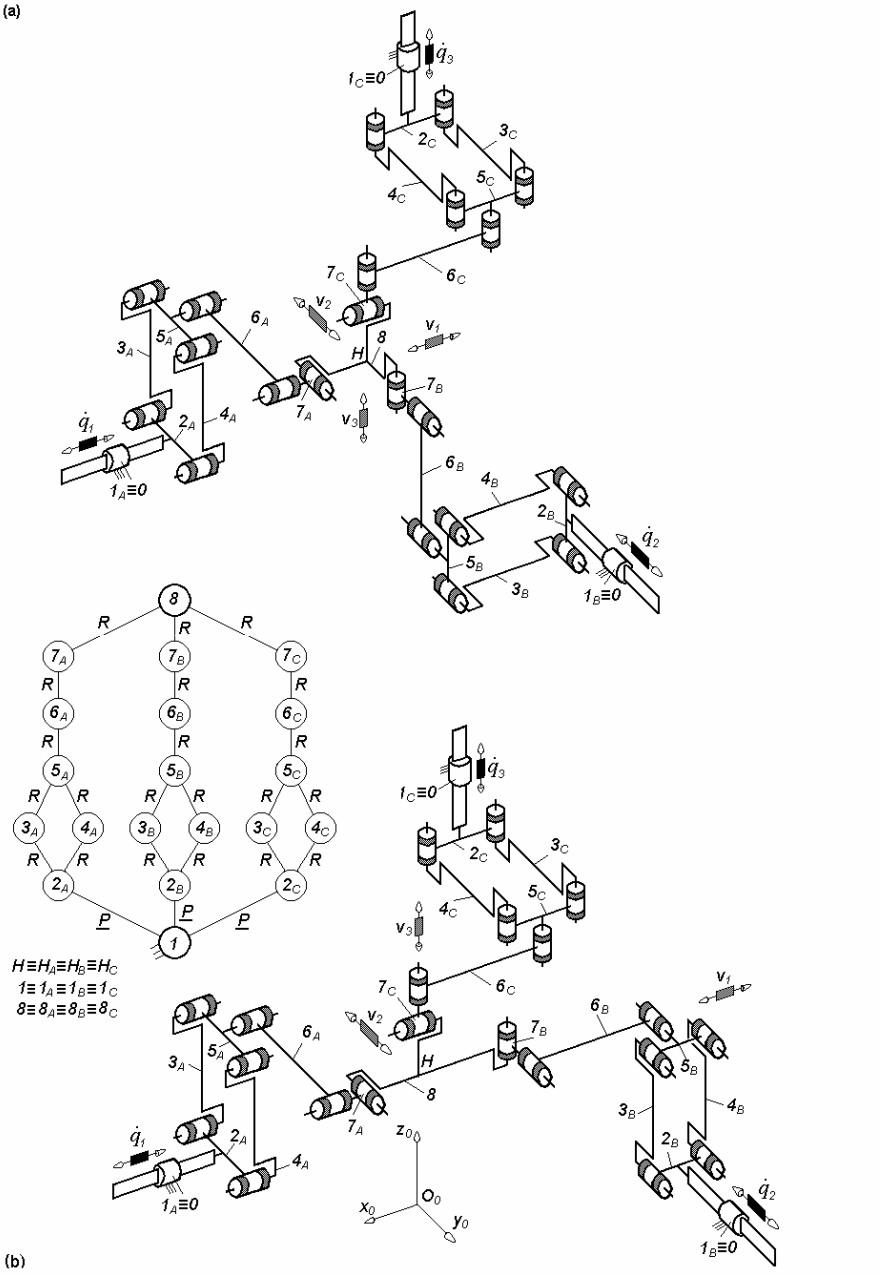

Fig. 7.24. *3-PPaRRR**-type overconstrained maximally-regular TPMs defined by $M_F = S_F = 3$, $(R_F) = (\boldsymbol{v}_1, \boldsymbol{v}_2, \boldsymbol{v}_3)$, $T_F = 0$, $N_F = 9$, limb topology $\underline{P}||Pa||R||R \perp R^*$

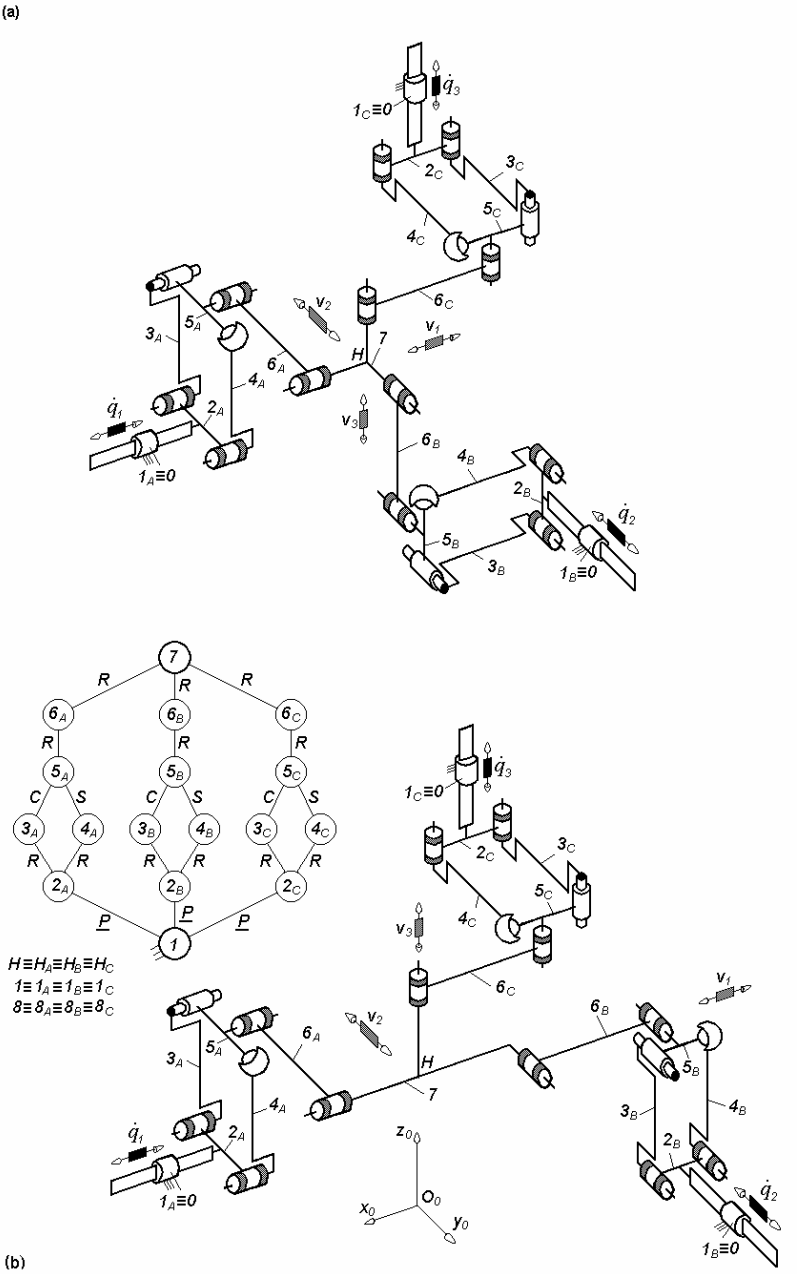

Fig. 7.25. *3-*$\underline{P}$*P*a^{cs}*RR*-type overconstrained maximally-regular TPMs defined by $M_F = S_F = 3$, $(R_F) = (\boldsymbol{v}_1, \boldsymbol{v}_2, \boldsymbol{v}_3)$, $T_F = 0$, $N_F = 3$, limb topology $\underline{P}||Pa^{cs}||R||R$

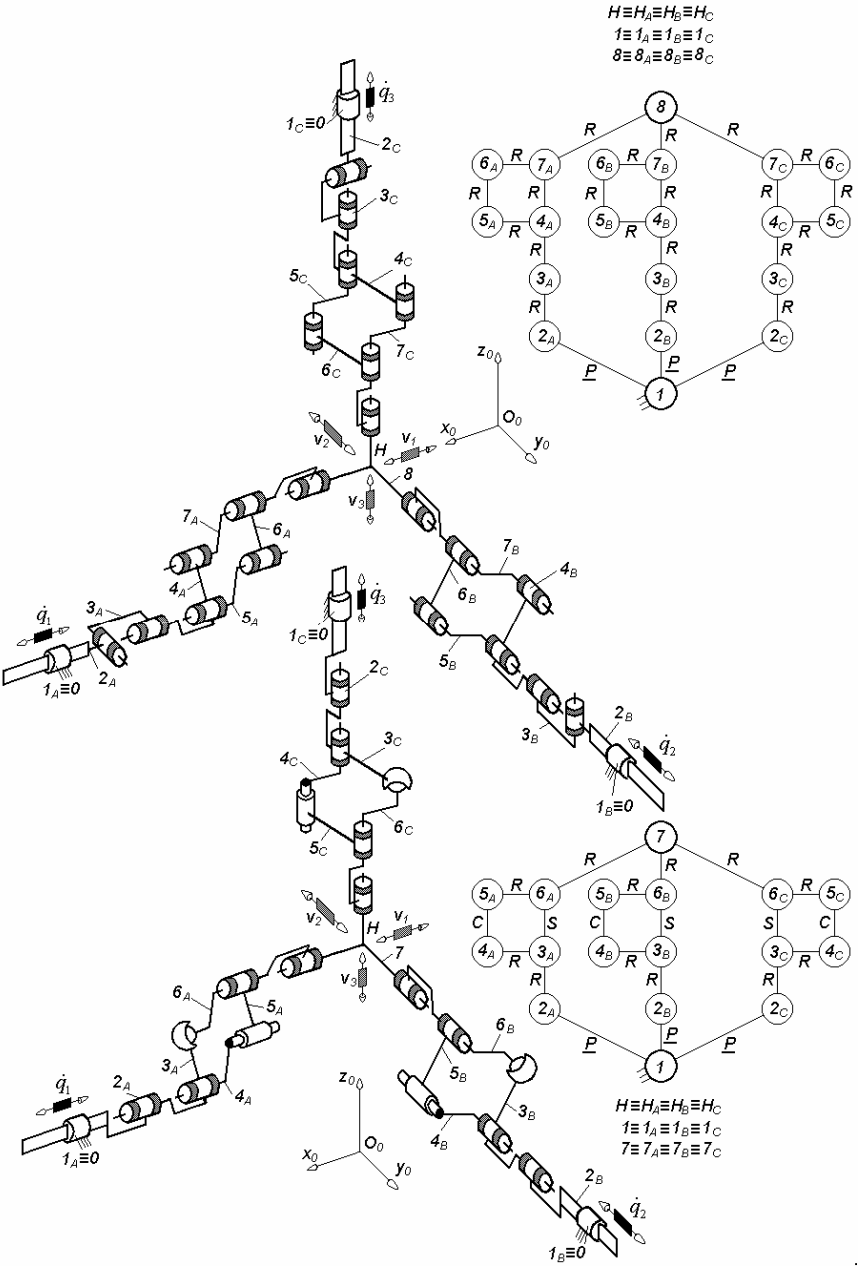

Fig. 7.26. Overconstrained maximally-regular TPMs of types *3-*$\underline{P}$*R*RRbR* (**a**) and *3-*$\underline{P}$*RRb*^{cs}*R* (**b**) defined by $M_F = S_F = 3$, $(R_F) = (\boldsymbol{v}_1, \boldsymbol{v}_2, \boldsymbol{v}_3)$, $T_F = 0$, $N_F = 9$ (**a**), $N_F = 3$ (**b**), limb topology $\underline{P} \perp R^* \perp {}^{||}R||Rb||R$ (**a**) and $\underline{P}||R||Rb^{cs}||R$ (**b**)

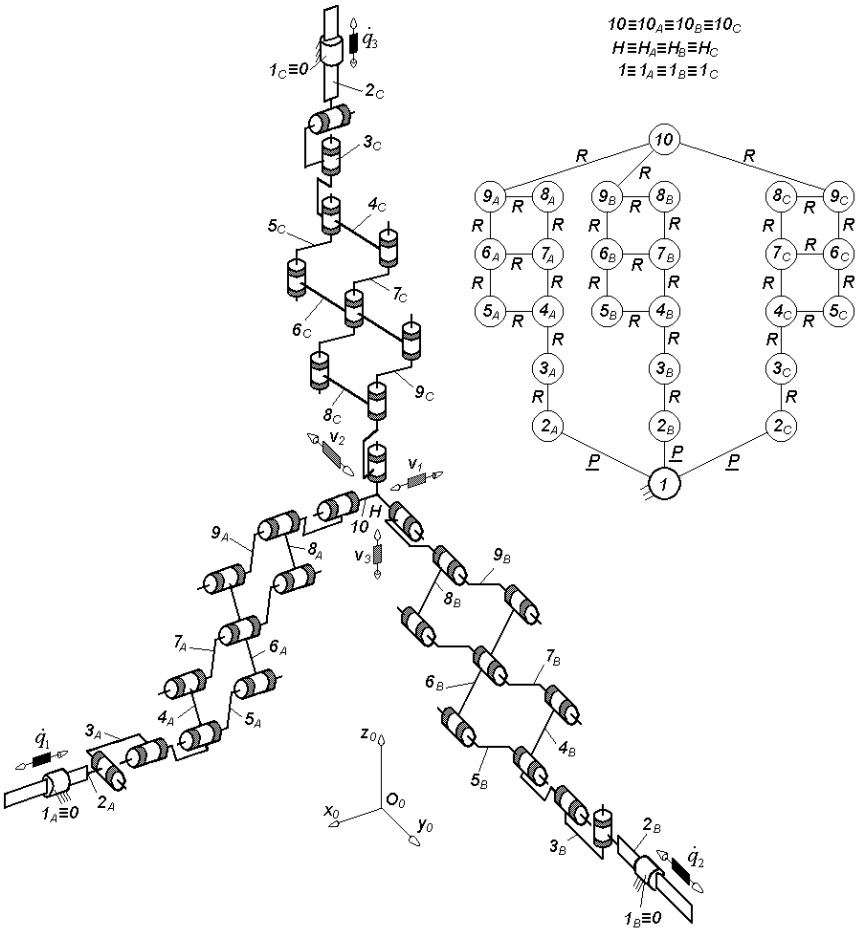

Fig. 7.27. *3-PR*RRbRbR*-type overconstrained maximally-regular TPM defined by $M_F = S_F = 3$, $(R_F) = (\boldsymbol{v}_1, \boldsymbol{v}_2, \boldsymbol{v}_3)$, $T_F = 0$, $N_F = 18$, limb topology $\underline{P} \perp R^* \perp {}^{||}R||Rb||Rb||R$

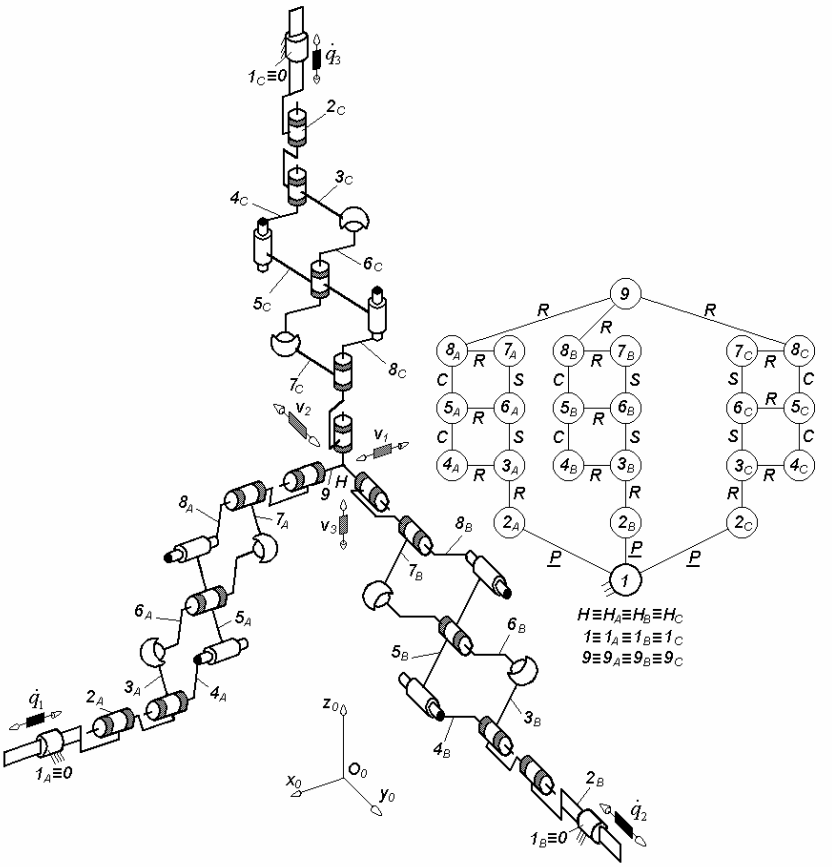

Fig. 7.28. *3-*$\underline{P}RRb^{cs}Rb^{cs}R$*-*type overconstrained maximally-regular TPM defined by $M_F = S_F = 3$, $(R_F) = (\boldsymbol{v}_1, \boldsymbol{v}_2, \boldsymbol{v}_3)$, $T_F = 0$, $N_F = 3$, limb topology $\underline{P}||R||Rb^{cs}||Rb^{cs}||R$

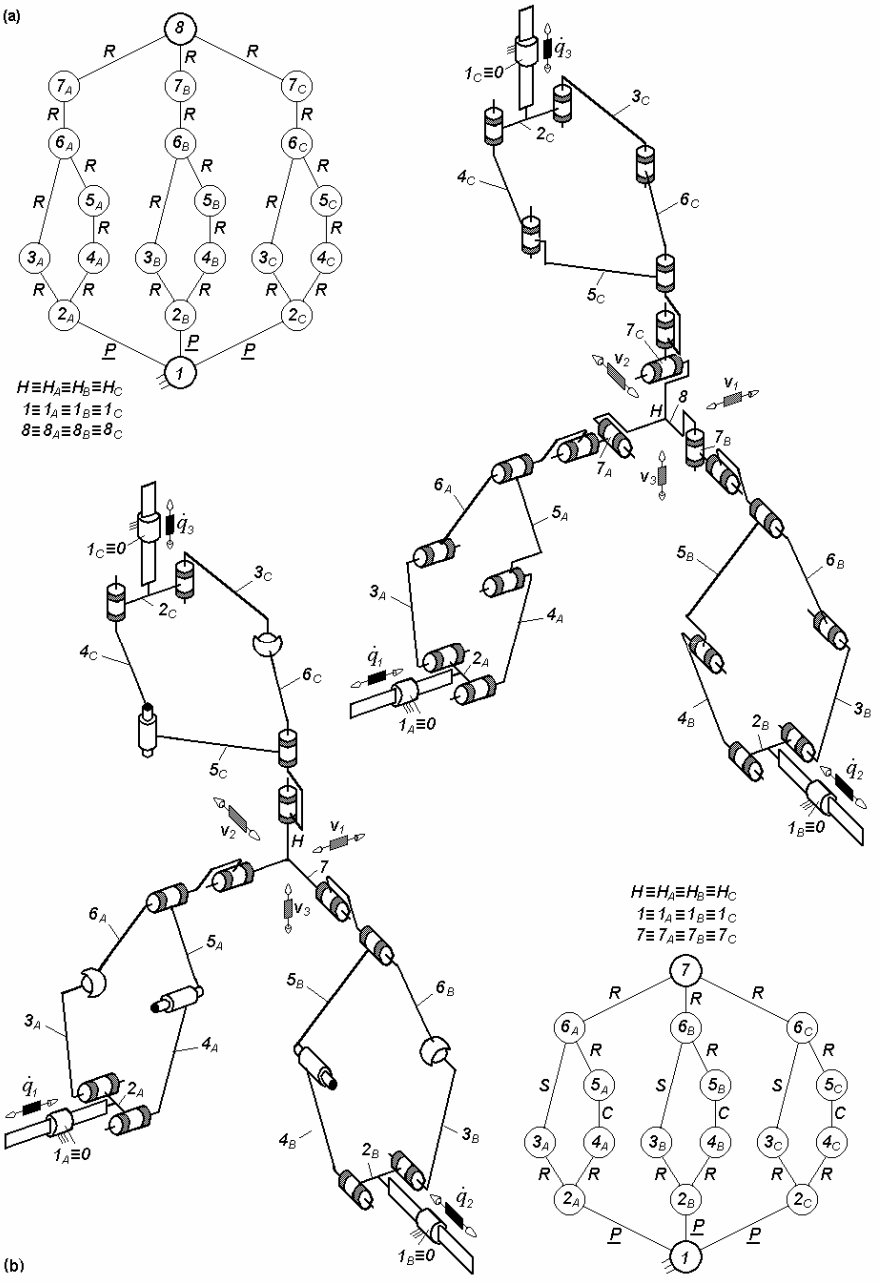

Fig. 7.29. Overconstrained maximally-regular TPMs of types *3-PPn2RR** (**a**) and *3-PPn2^{cs}R* (**b**) defined by $M_F = S_F = 3$, $(R_F) = (\boldsymbol{v}_1, \boldsymbol{v}_2, \boldsymbol{v}_3)$, $T_F = 0$, $N_F = 9$ (**a**), $N_F = 3$ (**b**), limb topology $\underline{P}||Pn2||R \perp R^*$ (**a**) and $\underline{P}||Pn2^{cs}||R$ (**b**)

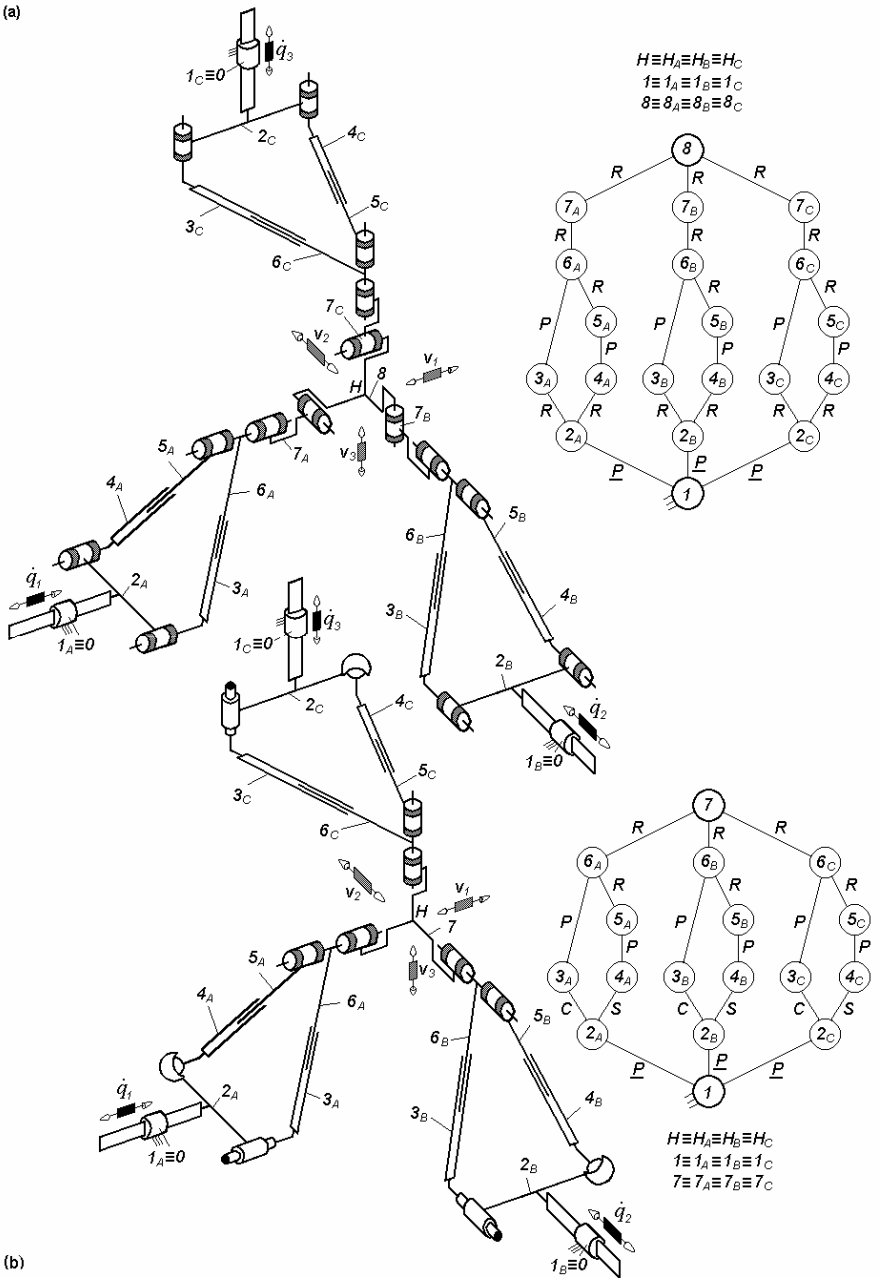

Fig. 7.30. Overconstrained maximally-regular TPMs of types *3-PPn2RR** (**a**) and *3-PPn2^{cs}R* (**b**) defined by $M_F = S_F = 3$, $(R_F) = (\boldsymbol{v}_1, \boldsymbol{v}_2, \boldsymbol{v}_3)$, $T_F = 0$, $N_F = 9$ (**a**), $N_F = 3$ (**b**), limb topology $\underline{P}||Pn2||R \perp R^*$ (**a**) and $\underline{P}||Pn2^{cs}||R$ (**b**)

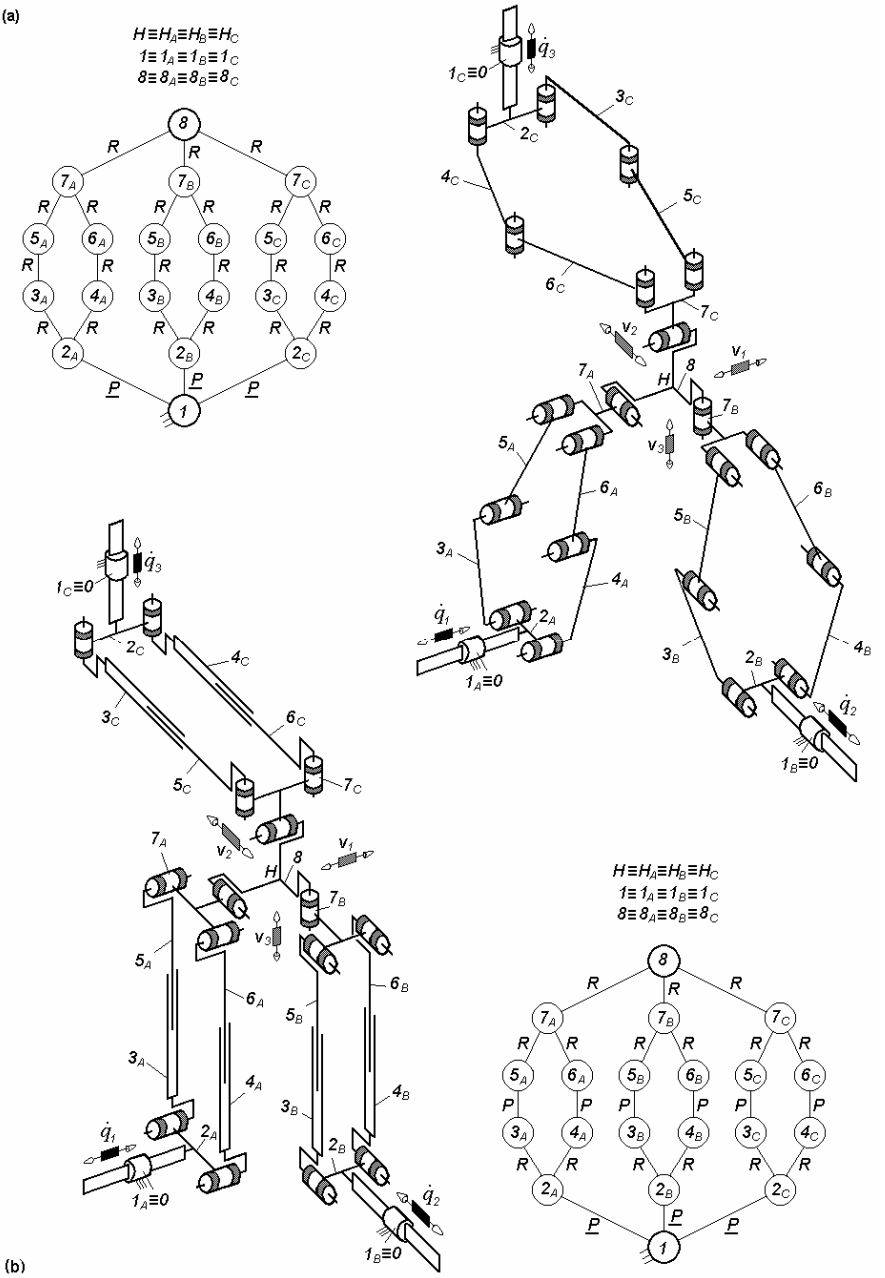

Fig. 7.31. *3-PPn3R**-type overconstrained maximally-regular TPMs defined by $M_F = S_F = 3$, $(R_F) = (\boldsymbol{v}_1, \boldsymbol{v}_2, \boldsymbol{v}_3)$, $T_F = 0$, $N_F = 9$, limb topology $\underline{P}||Pn3 \perp R^*$

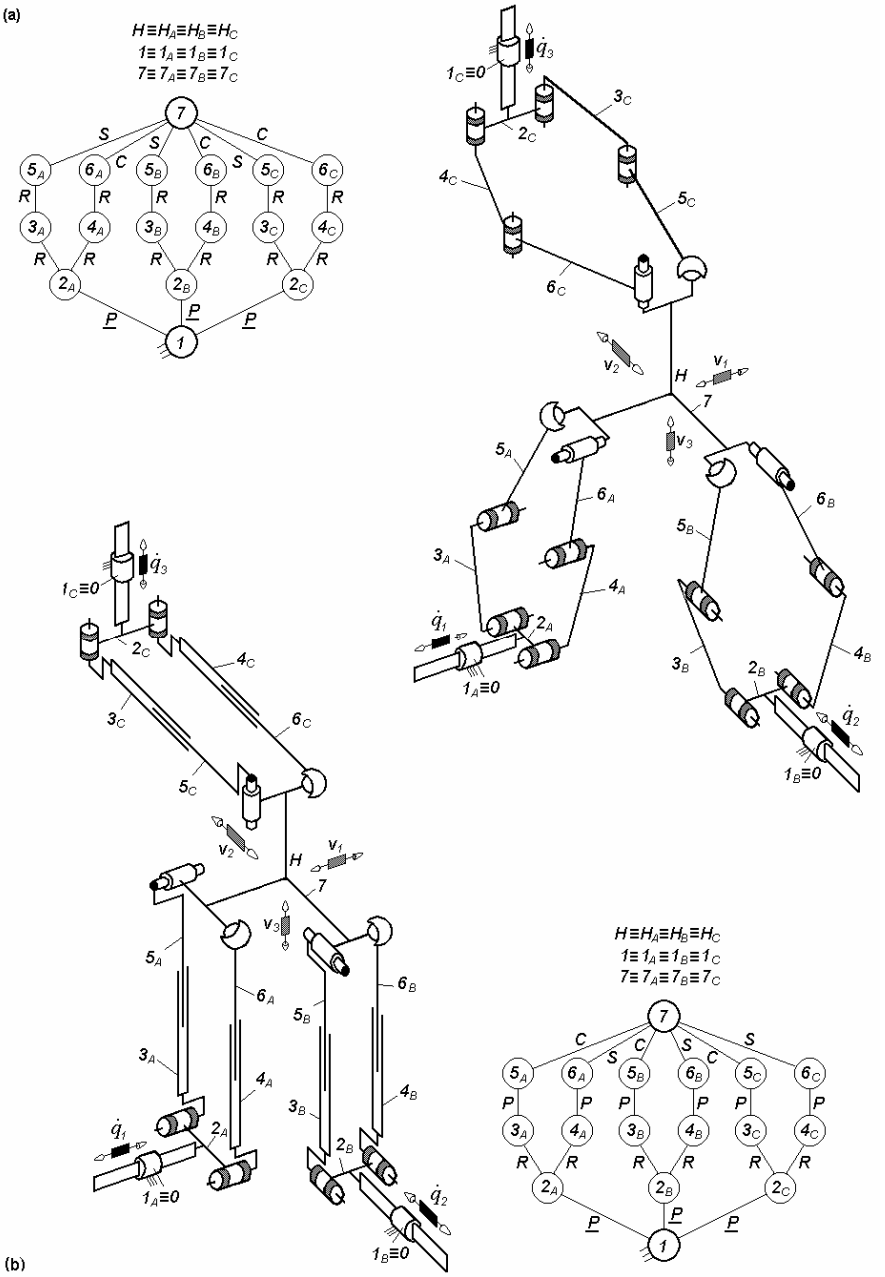

Fig. 7.32. *3-*$\underline{P}$*Pn3*^{cs}-type overconstrained maximally-regular TPMs defined by $M_F = S_F = 3$, $(R_F) = (\boldsymbol{v}_1, \boldsymbol{v}_2, \boldsymbol{v}_3)$, $T_F = 0$, $N_F = 3$, limb topology $\underline{P}||Pn3^{cs}$

7.2 Non overconstrained solutions

Equation (1.15) indicates that *non overconstrained* solutions of the maximally regular TPMs with q independent loops meet the condition $\sum_1^p f_i = 3 + 6q$ along with $M_F = S_F = 3$ and $(R_F) = (\boldsymbol{v}_1, \boldsymbol{v}_2, \boldsymbol{v}_3)$. They could have identical limbs or limbs with different topologies that may be actuated by linear motors.

In the non overconstrained maximally regular TPMs $F \leftarrow G_1$–G_2–G_3, the moving platform $n \equiv n_{Gi}$ $(i = 1, 2, 3)$ is connected to the reference platform $1 \equiv 1_{Gi} \equiv 0$ by three limbs with five degrees of connectivity. These solutions are derived from the overconstrained solutions presented in Figs. 7.3–7.32 by introducing the required idle mobilities.

For example, the non overconstrained solution in Fig. 7.33a is derived from the overconstrained solution in Fig. 7.3a by replacing, in each limb, two prismatic joints by cylindrical joints.

The bases of the operational velocities spaces of the limbs isolated from the parallel mechanisms presented in Figs. 7.33–7.45 are given in Table 7.10. The limb topology and connecting conditions of these solutions are systematized in Table 7.11 and the structural parameters of these solutions are presented in Tables 7.12–7.14.

Table 7.10. Bases of the operational velocities spaces of the limbs isolated from the parallel mechanisms presented in Figs. 7.33–7.45

No.	Parallel mechanism	Basis (R_{G1})	(R_{G2})	(R_{G3})
1	Figs. 7.33, 7.36–7.38	$(\boldsymbol{v}_1, \boldsymbol{v}_2, \boldsymbol{v}_3, \boldsymbol{\omega}_\beta, \boldsymbol{\omega}_\delta)$	$(\boldsymbol{v}_1, \boldsymbol{v}_2, \boldsymbol{v}_3, \boldsymbol{\omega}_\alpha, \boldsymbol{\omega}_\delta)$	$(\boldsymbol{v}_1, \boldsymbol{v}_2, \boldsymbol{v}_3, \boldsymbol{\omega}_\alpha, \boldsymbol{\omega}_\beta)$
2	Figs. 7.34a, 7.35, 7.39b, 7.40–7.45	$(\boldsymbol{v}_1, \boldsymbol{v}_2, \boldsymbol{v}_3, \boldsymbol{\omega}_\alpha, \boldsymbol{\omega}_\beta)$	$(\boldsymbol{v}_1, \boldsymbol{v}_2, \boldsymbol{v}_3, \boldsymbol{\omega}_\beta, \boldsymbol{\omega}_\delta)$	$(\boldsymbol{v}_1, \boldsymbol{v}_2, \boldsymbol{v}_3, \boldsymbol{\omega}_\alpha, \boldsymbol{\omega}_\delta)$
3	Fig. 7.39a	$(\boldsymbol{v}_1, \boldsymbol{v}_2, \boldsymbol{v}_3, \boldsymbol{\omega}_\alpha, \boldsymbol{\omega}_\delta)$	$(\boldsymbol{v}_1, \boldsymbol{v}_2, \boldsymbol{v}_3, \boldsymbol{\omega}_\alpha, \boldsymbol{\omega}_\beta)$	$(\boldsymbol{v}_1, \boldsymbol{v}_2, \boldsymbol{v}_3, \boldsymbol{\omega}_\beta, \boldsymbol{\omega}_\delta)$

Table 7.11. Limb topology of the non overconstrained maximally regular TPMs presented in Figs. 7.33–7.45

No.	Basic TPM Type	N_F	Derived TPM with $N_F=0$ Type	Limb topology
1	*3-<u>P</u>PP* (Fig. 7.3a)	*6*	*3-<u>P</u>C*C** (Fig. 7.33)	$\underline{P} \perp C^* \perp^{\perp} C^*$
2	*3-<u>P</u>RRP* (Fig. 7.4a)	*3*	*3-<u>P</u>RRC** (Fig. 7.34a)	$\underline{P} \| \| R \| \| R \perp C^*$
3	*3-<u>P</u>RPR* (Fig. 7.4b)	*3*	*3-<u>P</u>RC*R* (Fig. 7.34b)	$\underline{P} \| \| R \perp C^* \perp^{\|\|} R$
4	*3-<u>P</u>PRR* (Fig. 7.5a)	*3*	*3-<u>P</u>C*RR* (Fig. 7.35a)	$\underline{P} \perp C^* \perp^{\|\|} R \| \| R$
5	*3-<u>P</u>RRR* (Fig. 7.5b)	*3*	*3-<u>P</u>R*RRR* (Fig. 7.35b)	$\underline{P} \perp R^* \perp^{\|\|} R \| \| R \| \| R$
6	*3-<u>P</u>PaP* (Fig. 7.6)	*15*	*3-<u>P</u>Pa^{ss}C** (Fig. 7.36)	$\underline{P} \| \| Pa^{ss} \perp C^*$
7	*3-<u>P</u>PPa* (Fig. 7.7)	*15*	*3-<u>P</u>C*Pa^{ss}* (Fig. 7.37)	$\underline{P} \perp C^* \perp^{\|\|} Pa^{ss}$
8	*3-<u>P</u>PaPa* (Fig. 7.8)	*24*	*3-<u>P</u>Pa^{ss}Pa^{ss}* (Fig. 7.38)	$\underline{P} \| \| Pa^{ss} \| \| Pa^{ss}$
9	*3-<u>P</u>RRPa* (Fig. 7.9)	*12*	*3-<u>P</u>RRPa^{ss}* (Fig. 7.39a)	$\underline{P} \| \| R \| \| R \| \| Pa^{ss}$
10			*3-<u>P</u>R*RRPa^{cs}* (Fig. 7.39b)	$\underline{P} \perp R^* \perp^{\|\|} R \| \| R \| \| Pa^{cs}$
11	*3-<u>P</u>PaRR* (Fig. 7.10)	*12*	*3-<u>P</u>Pa^{ss}RR* (Fig. 7.40a)	$\underline{P} \| \| Pa^{ss} \| \| R \| \| R$
12			*3-<u>P</u>Pa^{cs}RRR** (Fig. 7.40b)	$\underline{P} \| \| Pa^{cs} \| \| R \| \| R \perp R^*$
13	*3-<u>P</u>RRbR* (Fig. 7.11a)	*12*	*3-<u>P</u>R*RRb^{cs}R* (Fig. 7.41)	$\underline{P} \perp R \perp^{\|\|} Rb^{cs} \| \| R$
14	*3-<u>P</u>RRbRbR* (Fig. 7.11b)	*21*	*3-<u>P</u>R*RRb^{cs}Rb^{cs}R* (Fig. 7.42)	$\underline{P} \perp R \perp^{\|\|} Rb^{cs} \| \| Rb^{cs} \| \| R$
15	*3-<u>P</u>Pn2R* (Fig. 7.12a, b)	*12*	*3-<u>P</u>Pn2^{cs}RR** (Figs. 7.43, 7.44)	$\underline{P} \| \| Pn2^{cs} \| \| R \perp R^*$
16	*3-<u>P</u>Pn3* (Fig. 7.13a, b)	*12*	*3-<u>P</u>Pn3^{cs}RR** (Fig. 7.45a, b)	$\underline{P} \| \| Pn3^{cs} \perp R^*$

Table 7.12. Structural parameters[a] of translational parallel mechanisms in Figs. 7.33–7.37

No.	Structural parameter	Solution *3-PC*C** (Fig. 7.33)	*3-PRRC** (Fig. 7.34a) *3-PRC*R* (Fig. 7.34b) *3-PC*RR* (Fig. 7.35a) *3-PR*RRR* (Fig. 7.35b)	*3-PPa^{ss}C** (Fig. 7.36) *3-PC*Pa^{ss}* (Fig. 7.37)
1	m	8	11	14
2	p_1	3	4	6
3	p_2	3	4	6
4	p_3	3	4	6
5	p	9	12	18
6	q	2	2	5
7	k_1	3	3	0
8	k_2	0	0	3
9	k	3	3	3
10	(R_{Gi}) $(i = 1,2,3)$	See Table 7.10	See Table 7.10	See Table 7.10
11	S_{G1}	5	5	5
12	S_{G2}	5	5	5
13	S_{G3}	5	5	5
14	r_{G1}	0	0	6
15	r_{G2}	0	0	6
16	r_{G3}	0	0	6
17	M_{G1}	5	5	5
18	M_{G2}	5	5	5
19	M_{G3}	5	5	5
20	(R_F)	$(\boldsymbol{v}_1, \boldsymbol{v}_2, \boldsymbol{v}_3)$	$(\boldsymbol{v}_1, \boldsymbol{v}_2, \boldsymbol{v}_3)$	$(\boldsymbol{v}_1, \boldsymbol{v}_2, \boldsymbol{v}_3)$
21	S_F	3	3	3
22	r_1	0	0	18
23	r_F	12	12	30
24	M_F	3	3	3
25	N_F	0	0	0
26	T_F	0	0	0
27	$\sum_{j=1}^{p_1} f_j$	5	5	11
28	$\sum_{j=1}^{p_2} f_j$	5	5	11
29	$\sum_{j=1}^{p_3} f_j$	5	5	11
30	$\sum_{j=1}^{p} f_j$	15	15	33

[a]See footnote of Table 2.1 for the nomenclature of structural parameters

Table 7.13. Structural parameters[a] of translational parallel mechanisms in Figs. 7.38–7.41

No.	Structural parameter	Solution *3-$\underline{P}$P$a^{ss}Pa^{ss}$* (Fig. 7.38)	*3-$\underline{P}$RRPa^{ss}* (Fig. 7.39a) *3-$\underline{P}$Pa^{ss}RR* (Fig. 7.40a)	*3-$\underline{P}$R*RRPa^{cs}* (Fig. 7.39b) *3-$\underline{P}$Pa^{cs}RRR** (Fig. 7.40b) *3-$\underline{P}$R*RRb^{cs}R* (Fig. 7.41)
1	m	20	17	20
2	p_1	9	7	8
3	p_2	9	7	8
4	p_3	9	7	8
5	p	27	21	24
6	q	8	5	5
7	k_1	0	0	0
8	k_2	3	3	3
9	k	3	3	3
10	(R_{Gi}) (i = *1,2,3*)	See Table 7.10	See Table 7.10	See Table 7.10
11	S_{G1}	5	5	5
12	S_{G2}	5	5	5
13	S_{G3}	5	5	5
14	r_{G1}	12	6	6
15	r_{G2}	12	6	6
16	r_{G3}	12	6	6
17	M_{G1}	5	5	5
18	M_{G2}	5	5	5
19	M_{G3}	5	5	5
20	(R_F)	($\boldsymbol{v}_1,\boldsymbol{v}_2,\boldsymbol{v}_3$)	($\boldsymbol{v}_1,\boldsymbol{v}_2,\boldsymbol{v}_3$)	($\boldsymbol{v}_1,\boldsymbol{v}_2,\boldsymbol{v}_3$)
21	S_F	3	3	3
22	r_l	36	18	18
23	r_F	48	30	30
24	M_F	3	3	3
25	N_F	0	0	0
26	T_F	0	0	0
27	$\sum_{j=1}^{p_1} f_j$	17	11	11
28	$\sum_{j=1}^{p_2} f_j$	17	11	11
29	$\sum_{j=1}^{p_3} f_j$	17	11	11
30	$\sum_{j=1}^{p} f_j$	51	33	33

[a]See footnote of Table 2.1 for the nomenclature of structural parameters

Table 7.14. Structural parameters[a] of translational parallel mechanisms in Figs. 7.42–7.45

No.	Structural parameter	Solution *3-<u>P</u>R*RRb^{cs}Rb^{cs}R* (Fig. 7.42)	*3-<u>P</u>Pn2^{cs}RR** (Figs. 7.43, 7.44) *3-<u>P</u>Pn3^{cs}RR** (Fig. 7.45)
1	m	26	20
2	p_1	11	8
3	p_2	11	8
4	p_3	11	8
5	p	33	24
6	q	8	5
7	k_1	0	0
8	k_2	3	3
9	k	3	3
10	(R_{Gi}) $(i = 1,2,3)$	See Table 7.10	See Table 7.10
11	S_{G1}	5	5
12	S_{G2}	5	5
13	S_{G3}	5	5
14	r_{G1}	12	6
15	r_{G2}	12	6
16	r_{G3}	12	6
17	M_{G1}	5	5
18	M_{G2}	5	5
19	M_{G3}	5	5
20	(R_F)	$(\boldsymbol{v}_1, \boldsymbol{v}_2, \boldsymbol{v}_3)$	$(\boldsymbol{v}_1, \boldsymbol{v}_2, \boldsymbol{v}_3)$
21	S_F	3	3
22	r_1	36	18
23	r_F	48	30
24	M_F	3	3
25	N_F	0	0
26	T_F	0	0
27	$\sum_{j=1}^{p_1} f_j$	17	11
28	$\sum_{j=1}^{p_2} f_j$	17	11
29	$\sum_{j=1}^{p_3} f_j$	17	11
30	$\sum_{j=1}^{p} f_j$	51	33

[a]See footnote of Table 2.1 for the nomenclature of structural parameters

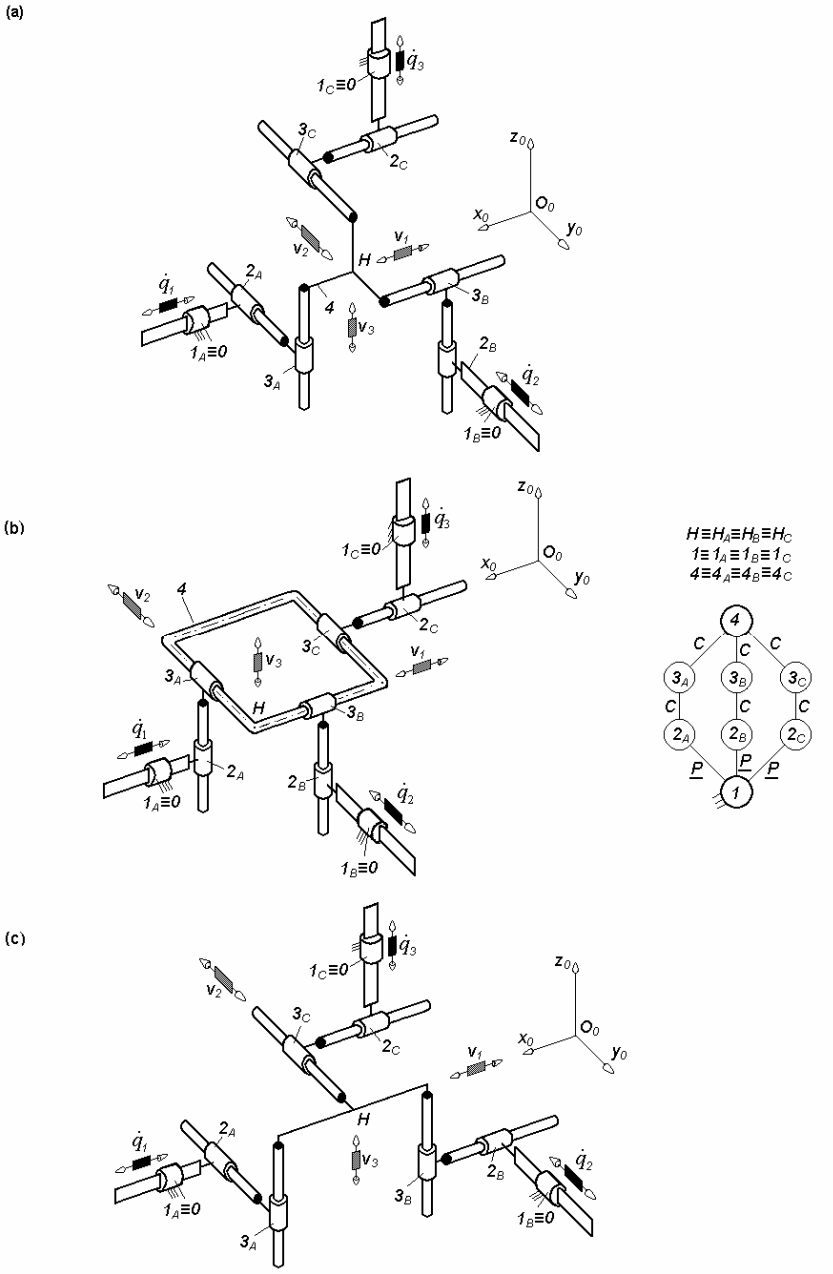

Fig. 7.33. *3-*$\underline{P}$*C*C**-type non overconstrained maximally regular TPMs, limb topology $\underline{P} \perp C^* \perp^{\perp} C^*$

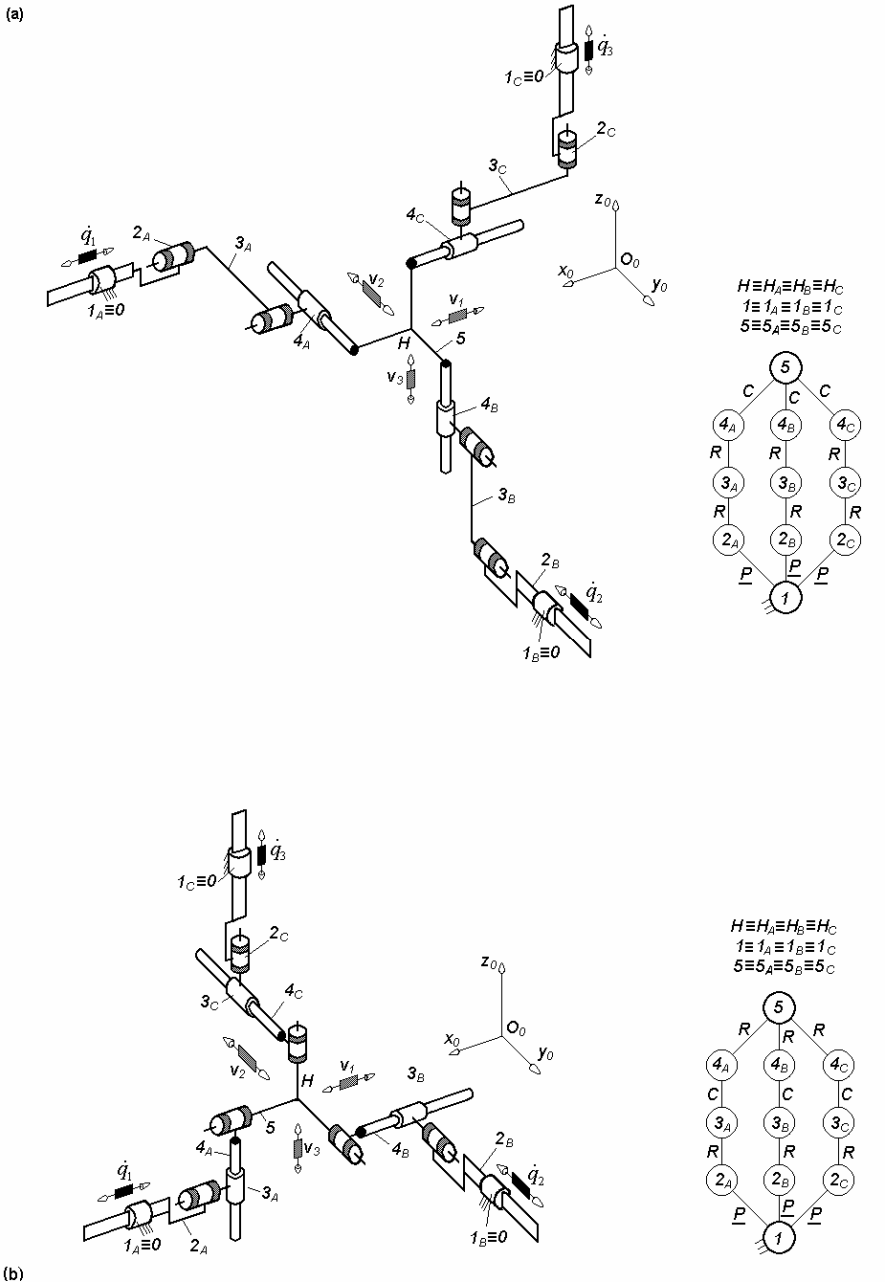

Fig. 7.34. Non overconstrained maximally regular TPMs of types *3-*$\underline{P}$*RRC** (**a**) and *3-*$\underline{P}$*RC*R* (**b**), limb topology $\underline{P}||R||R \perp C^*$ (**a**) and $\underline{P}||R \perp C^* \perp {}^{||}R$ (**b**)

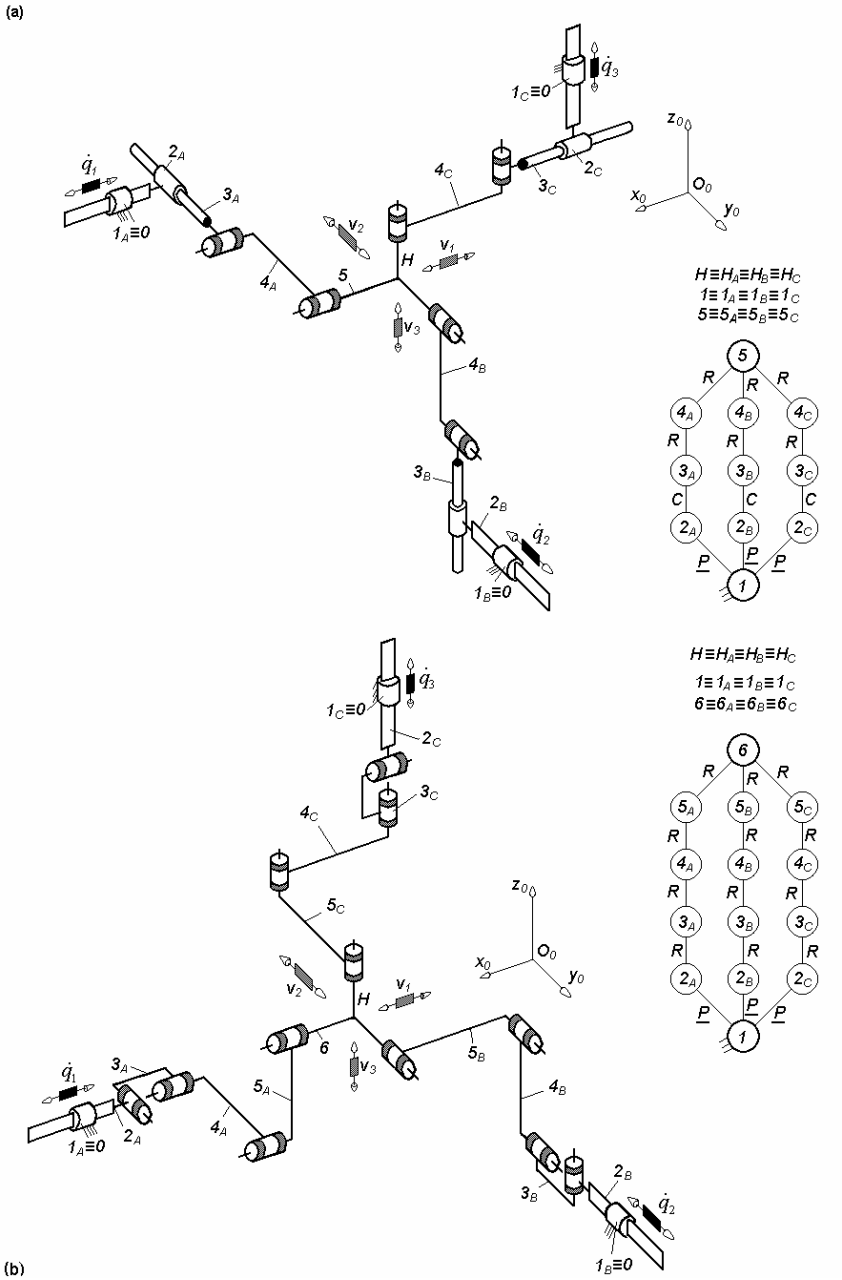

Fig. 7.35. Non overconstrained maximally regular TPMs of types *3-*$\underline{P}$*C*RR* (**a**) and *3-*$\underline{P}$*R*RRR* (**b**), limb topology $\underline{P} \perp C^* \perp {}^{||}R||R$ (**a**) and $\underline{P} \perp R^* \perp {}^{||}R||R||R$ (**b**)

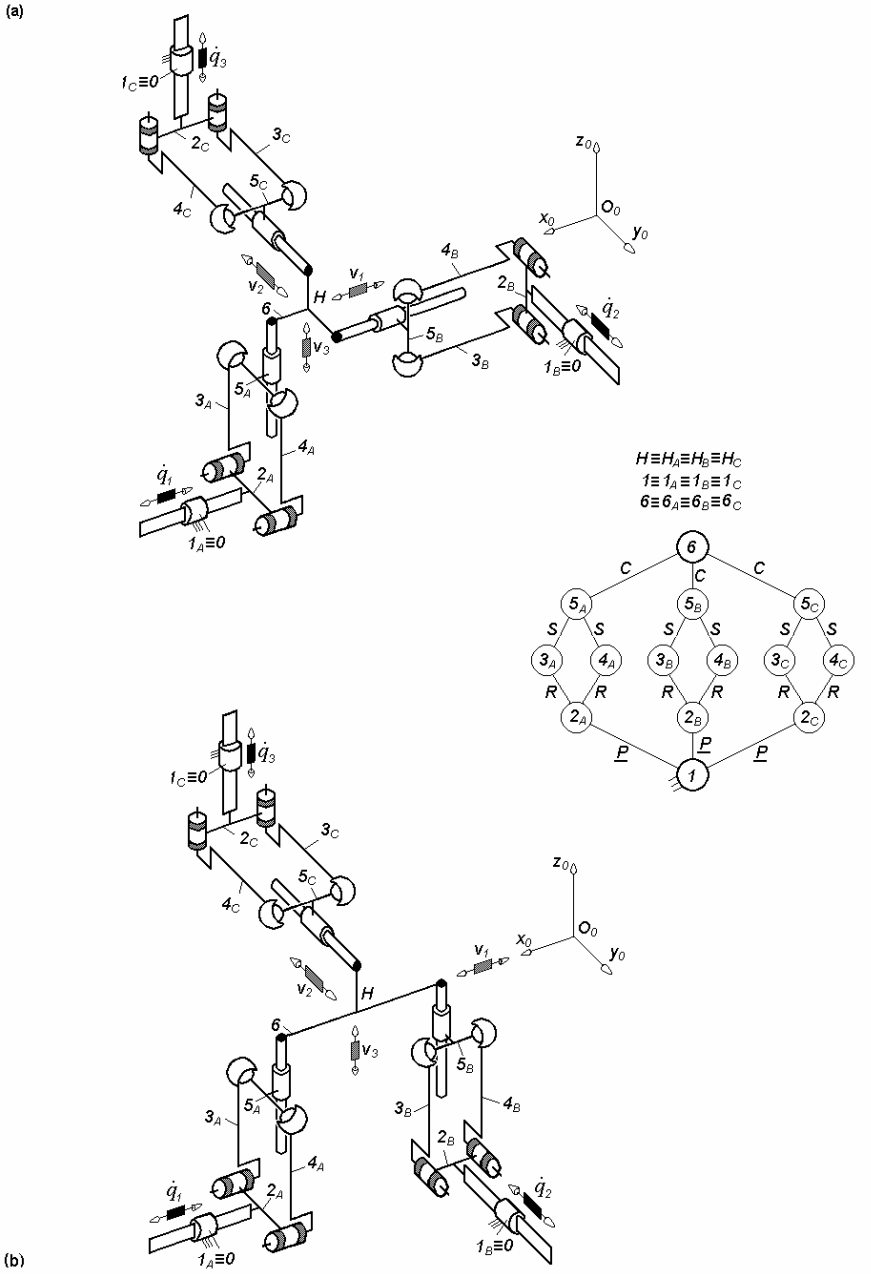

Fig. 7.36. *3-PPa^{ss}C**-type non overconstrained maximally-regular TPMs, limb topology $\underline{P}||Pa^{ss} \perp C^*$

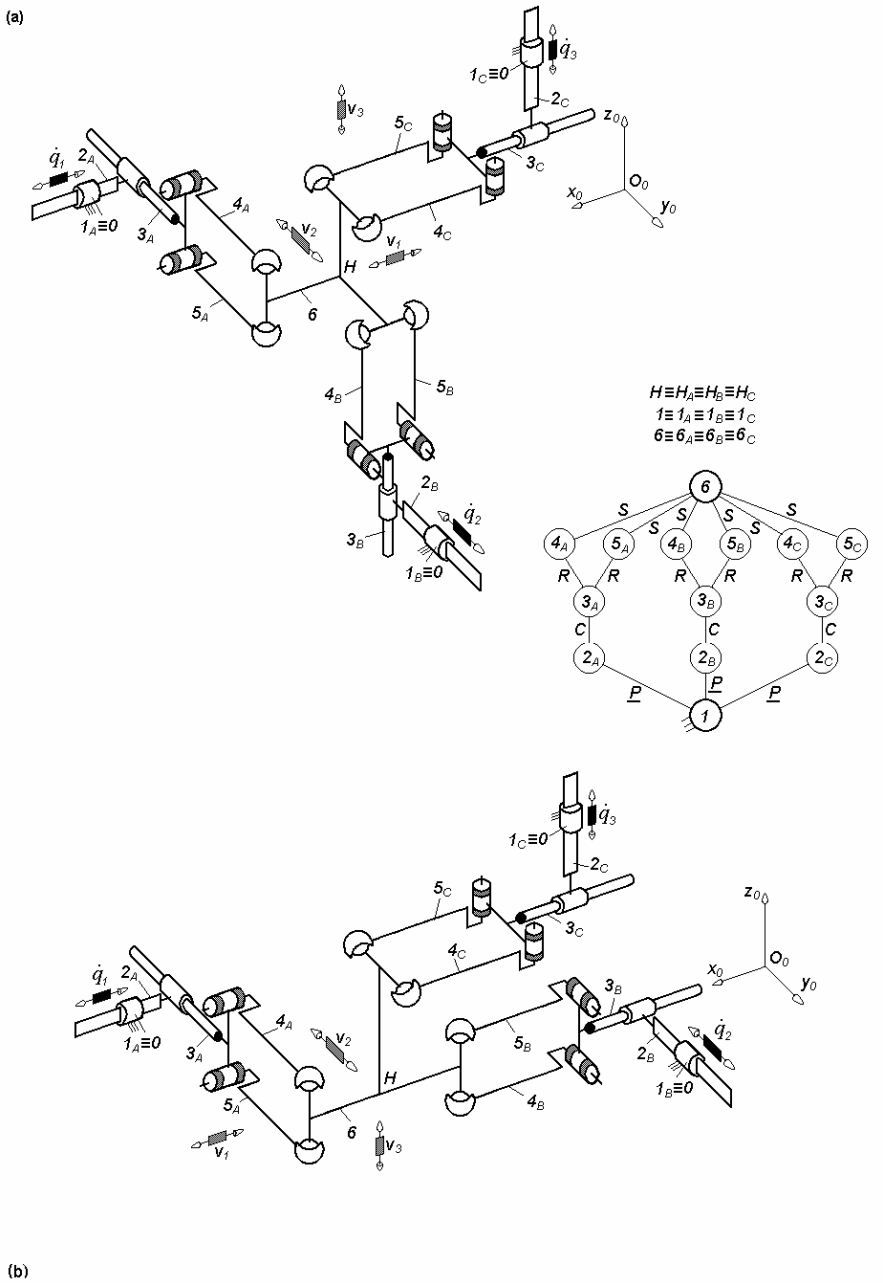

Fig. 7.37. *3-*$\underline{P}C^*Pa^{ss}$-type non overconstrained maximally-regular TPMs, limb topology $\underline{P} \perp C^* \perp {}^{\shortparallel}Pa^{ss}$

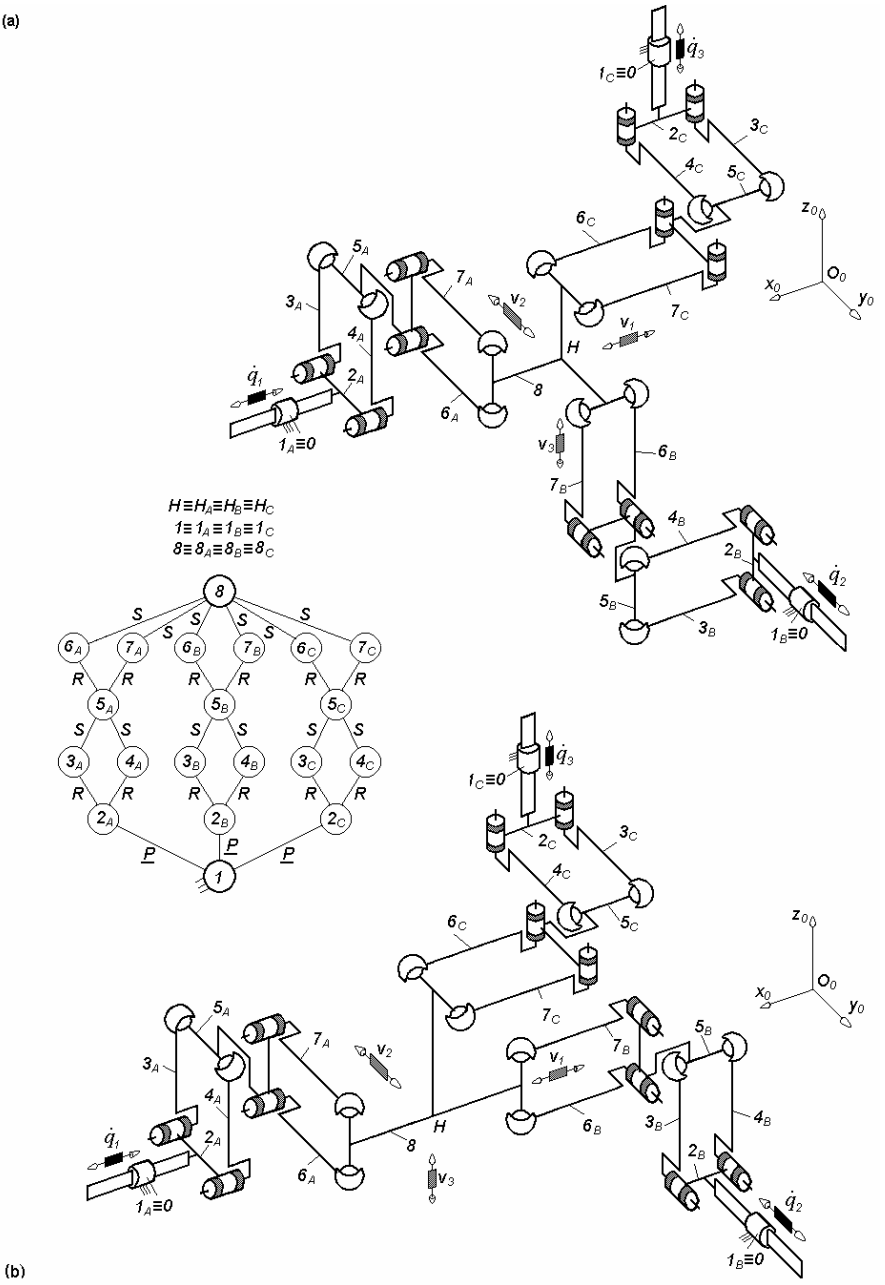

Fig. 7.38. *3-*$\underline{P}Pa^{ss}Pa^{ss}$-type non overconstrained maximally-regular TPMs, limb topology $\underline{P}||Pa^{ss}||Pa^{ss}$

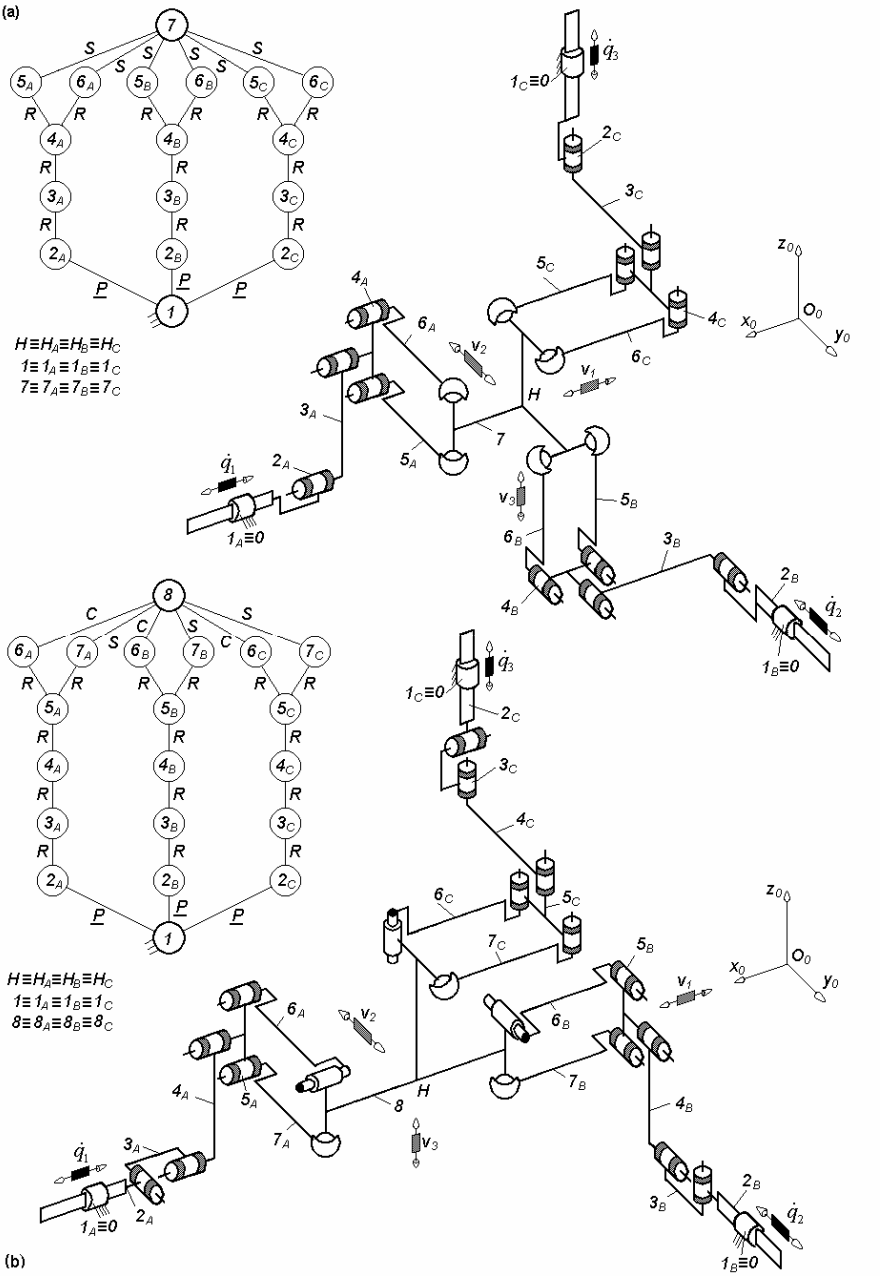

Fig. 7.39. Non overconstrained maximally-regular TPMs of types *3-*$\underline{P}$*RRPa*^{ss} (**a**) and *3-*$\underline{P}$*R*RRPa*^{cs} (**b**), limb topology $\underline{P}||R||R||Pa^{ss}$ (**a**) and $\underline{P} \perp R^* \perp {}^{||}R||R||Pa^{cs}$ (**b**)

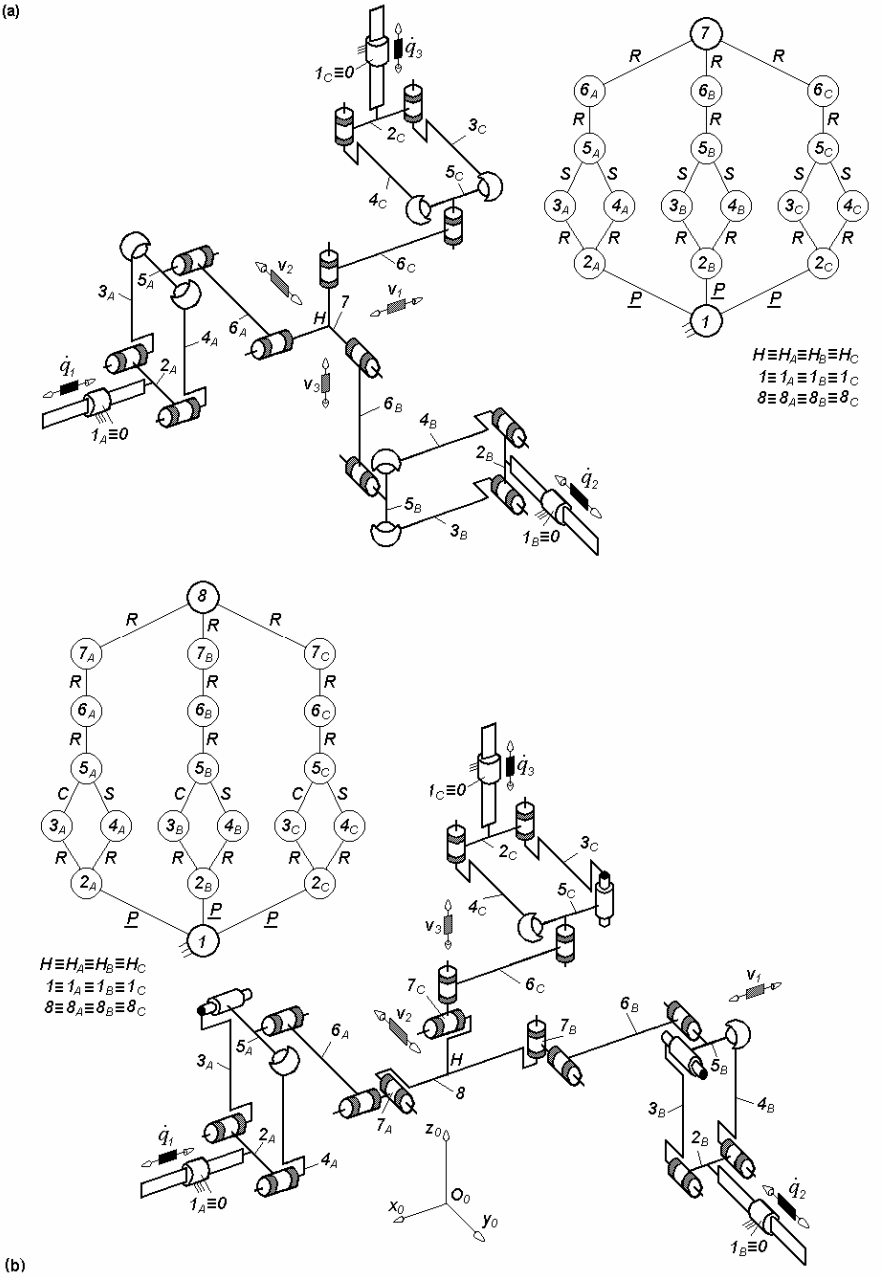

Fig. 7.40. Non overconstrained maximally-regular TPMs of types *3-*$\underline{P}$*PPa*^{ss}*RR* (**a**) and *3-*$\underline{P}$*PPa*^{cs}*RRR** (**b**), limb topology $\underline{P}||Pa^{ss}||R||R$ (**a**) and $\underline{P}||Pa^{cs}||R||R \perp R^*$ (**b**)

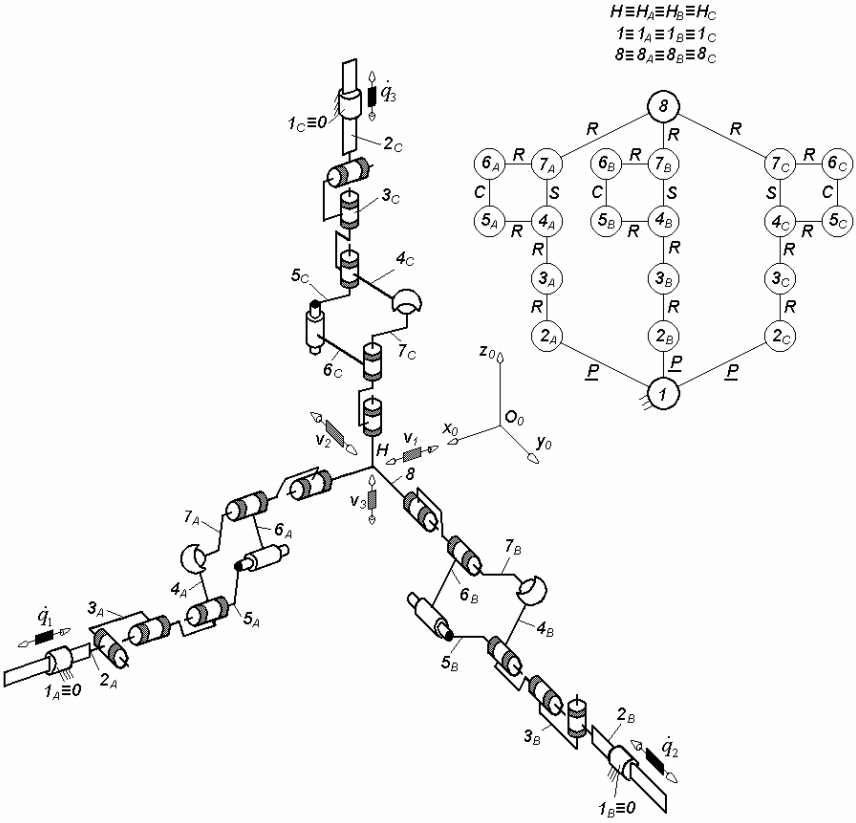

Fig. 7.41. *3-*$\underline{P}$*R*RRb*^{cs}*R*-type non overconstrained maximally-regular TPM, limb topology $\underline{P} \perp R \perp {}^{\parallel}Rb^{cs}\|R$

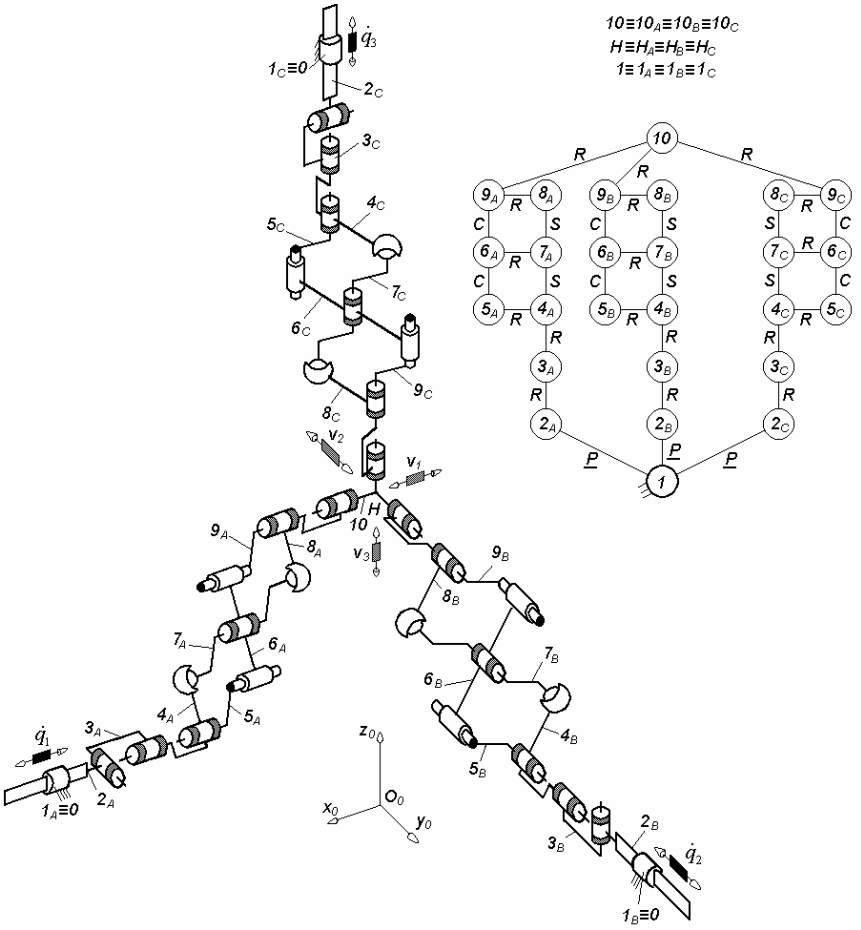

Fig. 7.42. *3-<u>P</u>R*RRb^{cs}Rb^{cs}R*-type non overconstrained maximally-regular TPM, limb topology $\underline{P} \perp R \perp {}^{||}Rb^{cs}||Rb^{cs}||R$

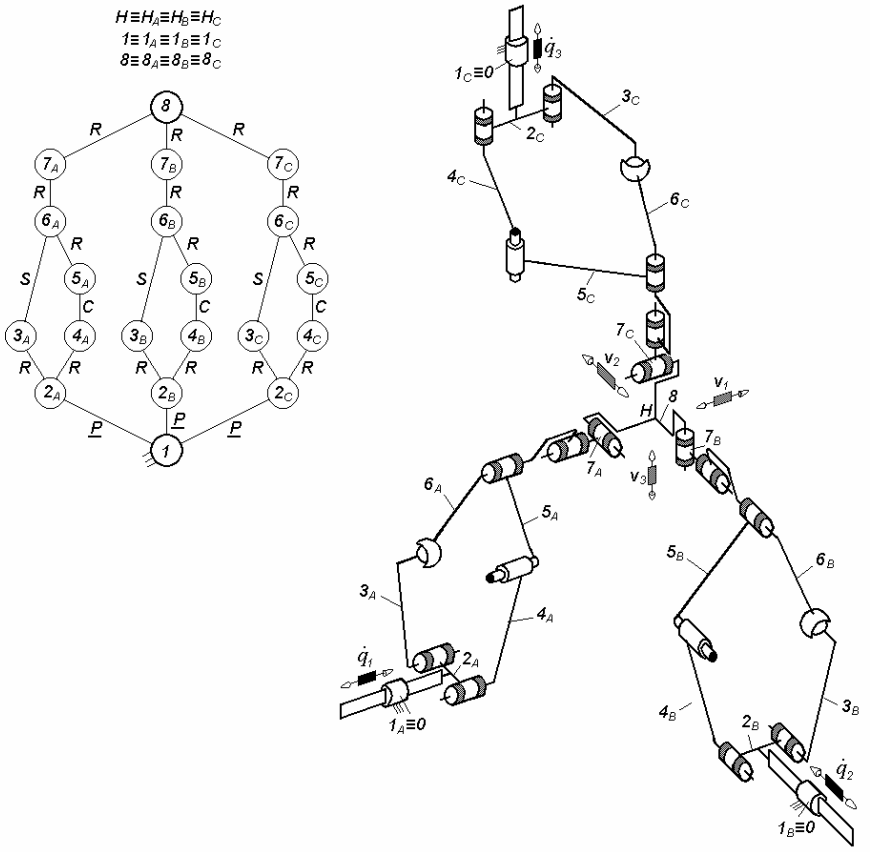

Fig. 7.43. *3-*$\underline{P}$*Pn2*^{cs}*RR**-type non overconstrained maximally-regular TPM, limb topology $\underline{P}||Pn2^{cs}||R \perp R$*

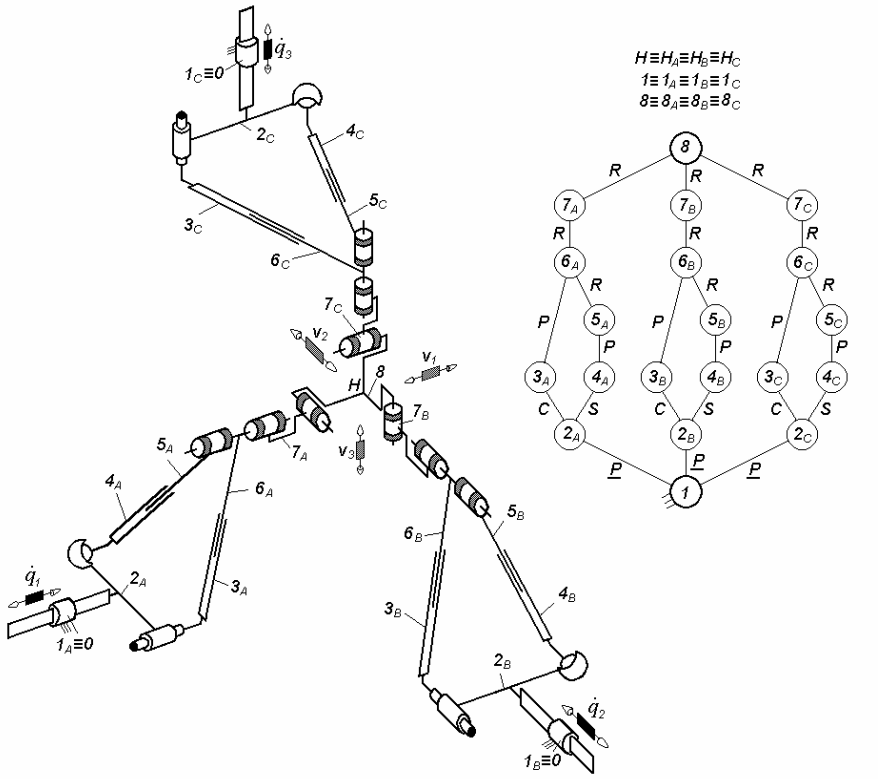

Fig. 7.44. *3-<u>P</u>Pn2^{cs}RR**-type non overconstrained maximally-regular TPM, limb topology $\underline{P}||Pn2^{cs}||R \perp R^*$

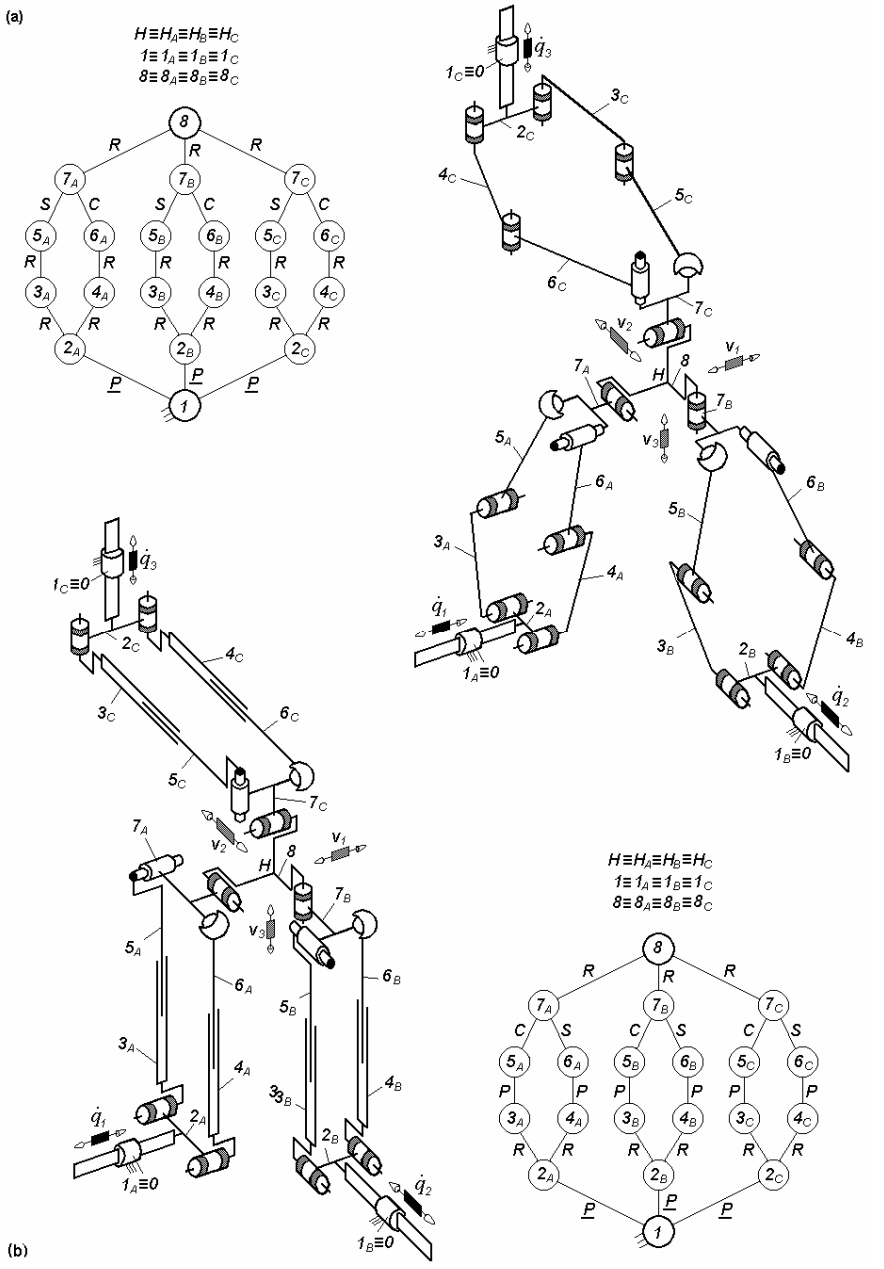

Fig. 7.45. *3-*$\underline{P}$*Pn3*^{cs}*RR**-type non overconstrained maximally-regular TPMs, limb topology $\underline{P} || Pn3^{cs} \perp R^*$

References

Alizade R, Bayram C (2004) Structural synthesis of parallel manipulators, Mech Mach Theory 39:857–870

Alizade R, Bayram C, Gezgin E (2007) Structural synthesis of serial platform manipulators. Mech Mach Theory 42:580–599

Angeles J (1997) Fundamentals of robotic mechanical systems: Theory, methods, and algorithms, Springer, New York

Badescu M, Morman J, Mavroidis CC (2002) Workspace optimization of 3-UPU parallel platforms with joint constraints. In: Proceedings of the IEEE International Conference on Robotics and Automation, pp 3678–3683

Bamberger H, Wolf A, Shoham M (2007) Architectures of translational parallel mechanism for MEMS fabrication. In: Proceedings of the 12th World Congress in Mechanism and Machine Science, Besançon

Baron L, Wang X, Cloutier G (2002) The isotropic conditions of parallel manipulators of Delta topology. In: Lenarčič J, Thomas F (eds) Advances in robot kinematics, Kluwer, Dordrecht, pp 357–366

Bergmeyer J (2002) Manipulator with two articulated arms. EP 1234642

Bleicher F, Günther G (2004) The 4th Chemnitz Parallel Kinematics Seminar, pp 165–181

Brogårdh T (2002) PKM research – important issues, presented as seen from a product development perspective at ABB Robotics. In: Gosselin CM, Ebert-Uphoff I (eds) Workshop on fundamental issues and future research directions for parallel mechanisms and manipulators, Quebec

Bruzzone LE, Molfino RM, Razzoli RP (2002) In: Proceedings of the IASTED International Conference on Modelling Identification and Control, Innsbruck, pp 518–522

Callegari M, Tarantini M (2003) Kinematic analysis of a novel translational platform. Trans ASME J Mech Design 125:308–315

Callegari M, Marzetti P (2003) Kinematics of a family of parallel translating mechanisms. In: Proceedings of RAAD'03 12th International Workshop on Robotics, Cassino

Caro S, Wanger P, Bennis F, Chablat D (2006) Sensitivity analysis of the Orthoglide, a 3-DOF Translational Parallel Kinematic Machine. Trans ASME J Mech Design 125:302–307

Carricato M, Parenti-Castelli V (2001) A family of 3-dof translational parallel manipulators. In: Proceedings of the 2001 ASME Design Engineering Technical Conference, DAC-21035, Pittsburgh